DP-1076

AEC RESEARCH AND DEVELOPMENT REPORT

ZERO-POWER MEASUREMENTS ON A HIGH-FLUX DEMONSTRATION LATTICE

A. E. DUNKLEE
C. E. JEWELL

DUPONT
REG. U.S. PAT. OFF.

Savannah River Laboratory

Aiken, South Carolina

LEGAL NOTICE

Printed in the United States of America
Available from
Clearinghouse for Federal Scientific and Technical Information
National Bureau of Standards, U. S. Department of Commerce
Springfield, Virginia 22151
Price: Printed Copy $3.00; Microfiche $0.65

664177

DP-1076

Reactor Technology
(TID-4500)

ZERO-POWER MEASUREMENTS ON A HIGH-FLUX DEMONSTRATION LATTICE

Albert E. Dunklee
Charles E. Jewell

Work done by

N. P. Baumann
F. D. Benton
A. E. Dunklee
W. E. Graves
C. E. Jewell
G. F. O'Neill
R. M. Satterfield
S. V. Topp

Approved by

J. L. Crandall, Research Manager
Experimental Physics Division

April 1967

E. I. DU PONT DE NEMOURS & COMPANY
SAVANNAH RIVER LABORATORY
AIKEN, S. C. 29801

CONTRACT AT(07-2)-1 WITH THE
UNITED STATES ATOMIC ENERGY COMMISSION

ABSTRACT

A Savannah River production reactor was loaded with a novel lattice capable of operation at neutron fluxes in excess of 6×10^{15} n/(cm^2)(sec). The high flux was attained by operating a relatively small number of fuel elements at very high specific powers to achieve maximum neutron production and by using a very light lattice to achieve long neutron lifetimes. The reactor control system was modified to compensate for fuel burnup and to provide optimum flux shaping.

In preparation for this new loading, experiments were performed in the SRL exponential (SE) and critical (PDP) facilities to specify the lattice design, the fuel concentrations, and the control rod types and configurations for the high-flux loading. A number of additional experiments determined the following operating and safety characteristics: temperature coefficients, void coefficients, light water coefficients, and flux distributions. A final zero-power critical test was made on the production lattice prior to its insertion into the production reactor.

CONTENTS

LIST OF TABLES

LIST OF FIGURES

INTRODUCTION

One of the production reactors (Figure 1) at the Savannah River Plant was modified for isotope production at high neutron flux (up to 6×10^{15} neutrons/(cm^2)(sec)). The lattice, shown in Figure 2, consisted of 108 tubular fuel assemblies (Figure 3) and 37 septifoil control assemblies (Figure 4), occupying a region 7 feet in diameter and 6 feet high in the center of the reactor tank. The lattice was moderated and cooled with D_2O and was surrounded by D_2O reflectors more than 3 feet thick. High flux was achieved by a combination of high specific power and light fuel loading.

Extensive physics experiments were performed in support of the high-flux design. Their purpose was threefold:

- To achieve the maximum neutron flux compatible with reasonably long core lifetimes.
- To provide adequate control and flux shaping capabilities.
- To maintain nuclear safety.

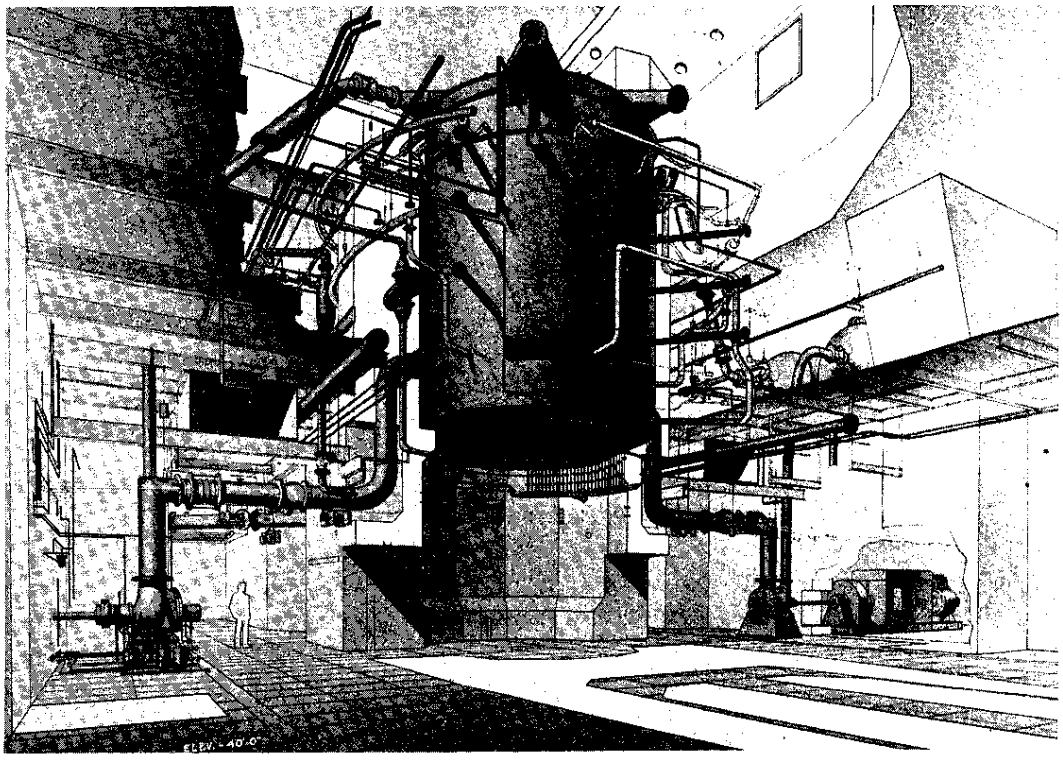

FIG. 1 SAVANNAH RIVER PRODUCTION REACTOR WITH CONCRETE SHIELDING CUT AWAY

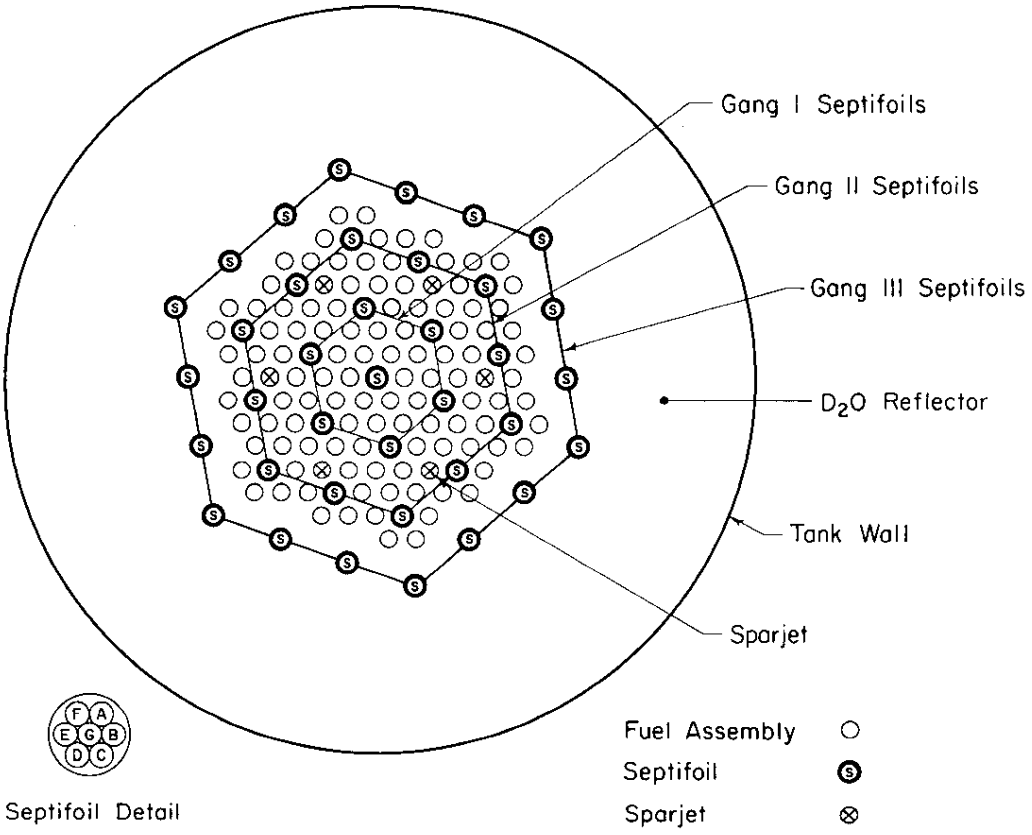

FIG. 2 HIGH-FLUX DEMONSTRATION LATTICE

Dimension, inches	
Outer housing, OD	3.420
Outer housing, ID	3.300
Clad outer fuel, OD	3.020
Bare outer fuel, OD	2.960
Bare outer fuel, ID	2.796
Clad outer fuel, ID	2.736
Clad inner fuel, OD	2.354
Bare inner fuel, OD	2.294
Bare inner fuel, ID	2.108
Clad inner fuel, ID	2.048
Inner housing, OD	1.740
Inner housing, ID	1.640

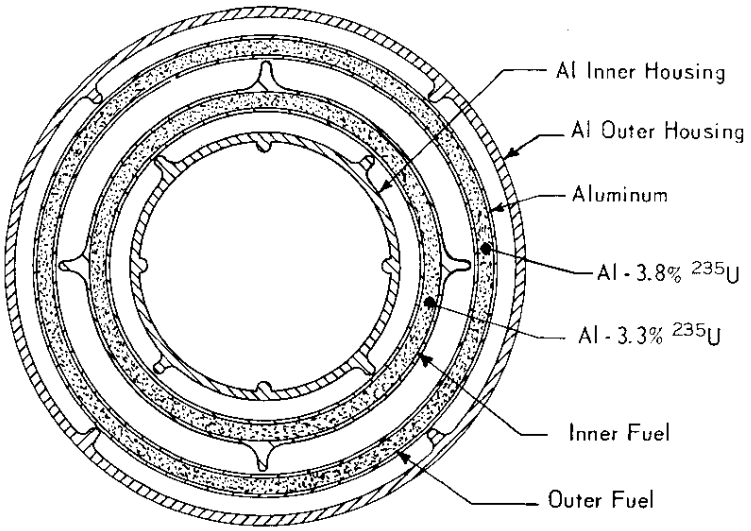

FIG. 3 HIGH-FLUX FUEL ASSEMBLY

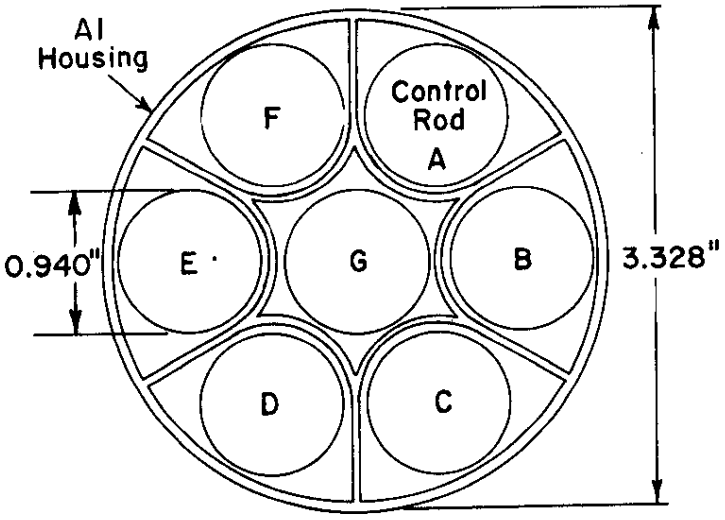

FIG. 4 CONTROL ROD CLUSTER

SUMMARY

The experiments were performed in three stages: (a) exponential experiments in the Subcritical Experiment (SE)[1], (b) critical experiments in the zero-power Process Development Pile (PDP)[2], and (c) a direct test of the full production lattice in the PDP just prior to charging of the production reactor.

(a) The exponential experiments served to verify the theoretical estimate that the desired ^{235}U concentration was about 25 g/ft, to measure the worth of a standard control system and the amount of flux distortion produced by the control rods, and to determine that the moderator temperature coefficient of reactivity was adequately negative. Auxiliary experiments were aimed at separating the effects of k_∞ changes, of control rod worth changes, and of neutron leakage on the temperature coefficient.

(b) The PDP mockup experiments provided more quantitative design information. The fuel concentration for the startup production lattice was established at 22.0 g of ^{235}U per linear foot of fuel assembly for a control rod complement consisting of seven small-diameter cadmium rods in each septifoil. The reactivity differential for the fuel concentration was established at ~70 μB per g ^{235}U/ft of fuel assembly. Similar differentials were obtained for a number of control rod designs. The moderator temperature coefficient of reactivity was measured to be -1.7 μB/°C,

and the prompt temperature coefficient (for uniform heating of the fuel assembly) was measured to be -0.3 μB/°C. The effect of adding H_2O to the coolant or to the moderator was to decrease the reactivity by about 10 or 100 μB/% H_2O, respectively. Other experiments in this mockup determined the worth of the "sparjets"(a) and of the irradiation targets, the flux ratios between different lattice components, and the flux variation with control rod manipulation. The response of external neutron instruments was strongly affected by the 18 septifoils located just outside the reactor core. Removal of control rods from these clusters gave an increase by a factor of four in the flux measured at the radial exterior ion chambers, even though the corresponding change in buckling was only about 80 μB.

(c) Measurements with the production load in the PDP established reactivity, control rod worths, and safety rod worths for this lattice. The latter were measured at 925 μB for all septifoils filled with three 0.45, two 0.35, and two 0.27-inch-diameter rods, and at 259 μB for all 27 safety rod positions filled with 0.35-inch-diameter cadmium rods.

A number of tests made in both the mockup and production loadings served to determine the kinetic response of the charge. This information is needed to analyze flux transient measurements by which the operating coefficients in the production reactors are determined.

DISCUSSION

Measurements of physics parameters for the high-flux demonstration lattice were carried out in three phases. First, partial mockups of various proposed cores were installed in the Subcritical Experiment (SE)[1], where bucklings, control rod worths, and temperature coefficients were measured. Following these studies, a full-scale mockup of the proposed core was installed in the Process Development Pile (PDP)[2] and a number of detailed measurements were carried out. Finally, a full production charge of fuel and control rods was installed in the PDP and used to verify the results of the earlier mockup experiments.

(a) D_2O discharge pipes used to improve moderator circulation (see Figure 2).

SUBCRITICAL MEASUREMENTS IN THE EXPONENTIAL FACILITY

The SE, one of the Savannah River exponential facilities, is illustrated in Figure 5. It consists of a D_2O-filled tank 5 feet in diameter and 7 feet high. The SE is mounted on a short graphite thermal column over the Standard Pile (SP)[3], which serves as its neutron source.

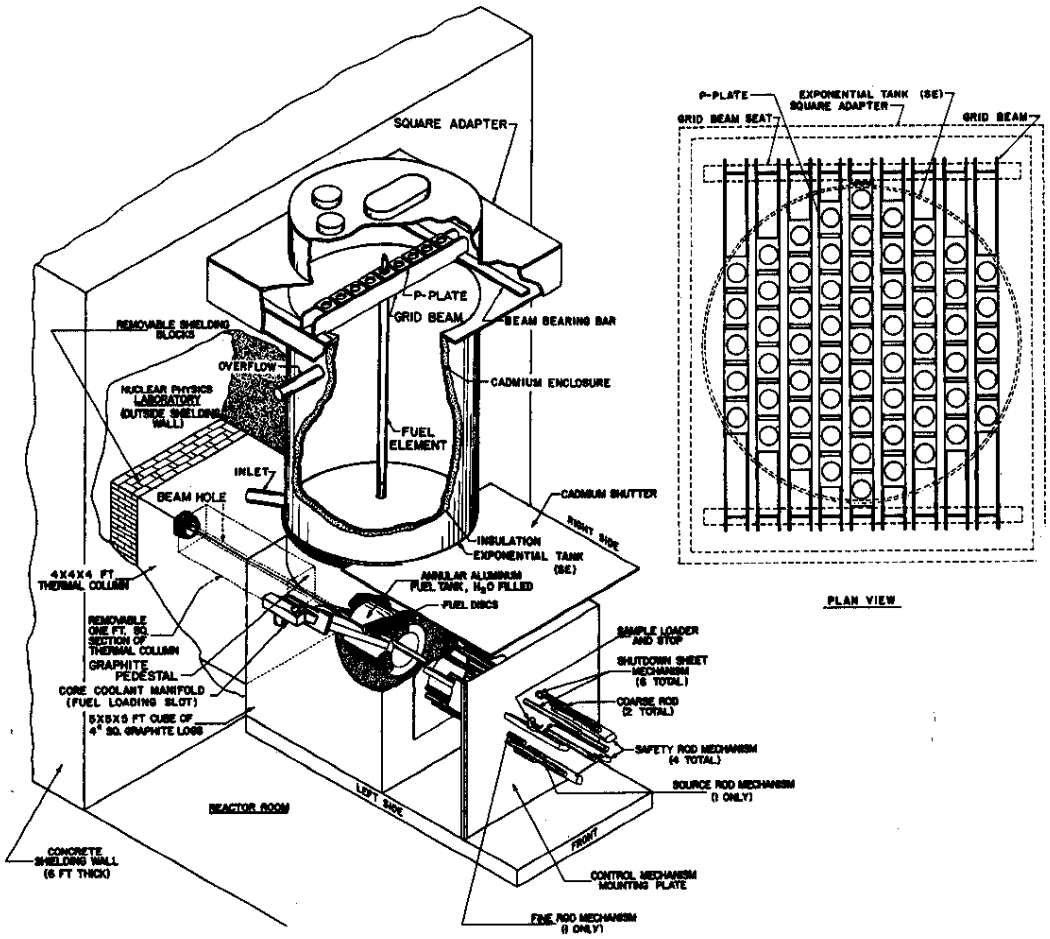

FIG. 5 SUBCRITICAL EXPERIMENT

The repeating lattice unit (referred to as a flat zone, or FZ, hex) in the high-flux load consists of six fuel assemblies surrounding a control cluster (septifoil) on a 7-inch triangular spacing. The SE is large enough to contain 61 lattice positions - 7 FZ hexes plus 12 extra fuel positions. A lattice diagram of an SE loading of a high-flux lattice is shown in Figure 6.

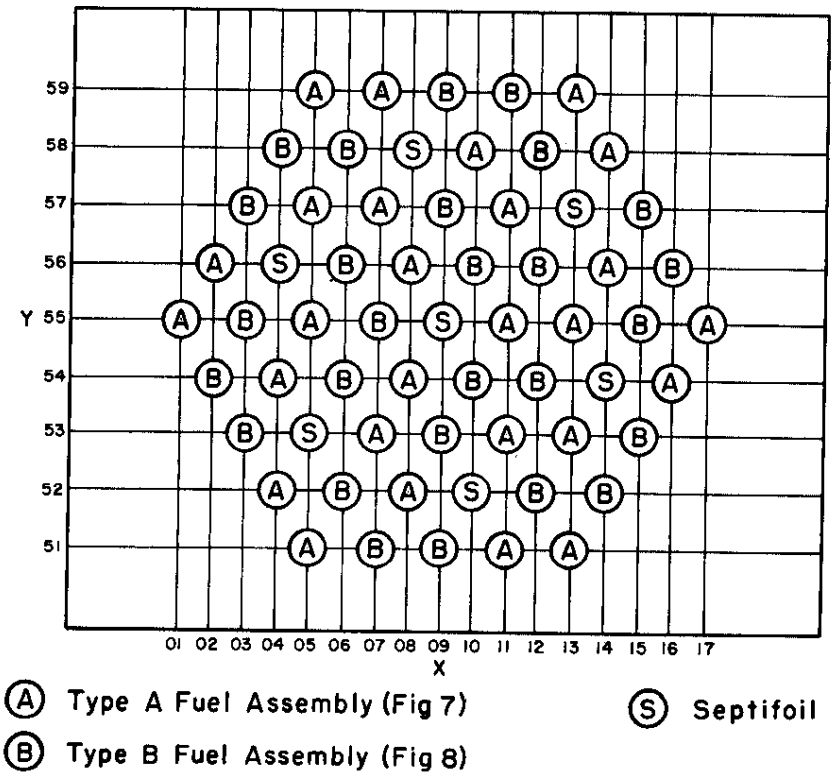

FIG. 6 SE MOCKUP OF HIGH-FLUX CORE

SE Fuel Mockup

Neither the design double-tube fuel assemblies of the type shown in Figure 3 nor cadmium control rods of proper diameters were available for the initial mockup studies in the SE. However, single ^{235}U aluminum tubes containing quantities of ^{235}U approximating the total amounts called for in the double tubes were available. Since it was expected that local neutron flux distortions in the high-flux lattice should be minor and that the bucklings and temperature coefficients should not be sensitive to the exact distribution of uranium and aluminum, the heavier single tubes were considered to be an adequate mockup of the lightly loaded double-tube fuel elements.

Similar considerations were used in selecting the control cluster mockups. The varying-diameter cadmium rods called for in the reference design were mocked up by a variety of lithium-aluminum and large-diameter cadmium rods covering the same range of absorption or relative "blackness." Details of the SE fuel assemblies are given in Figures 7 and 8, and similar information on the control rods is given in Figure 9. Locations of the various components in the SE lattice are shown in Figure 6.

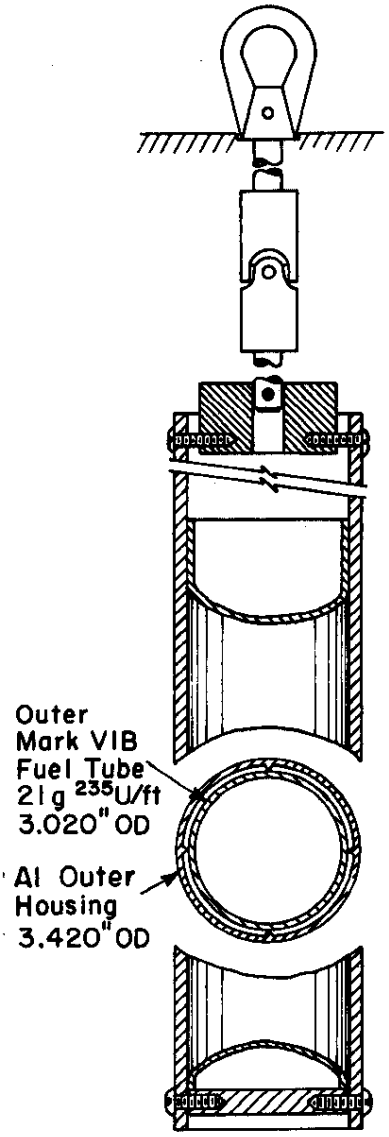

FIG. 7 SE FUEL ASSEMBLY-TYPE A

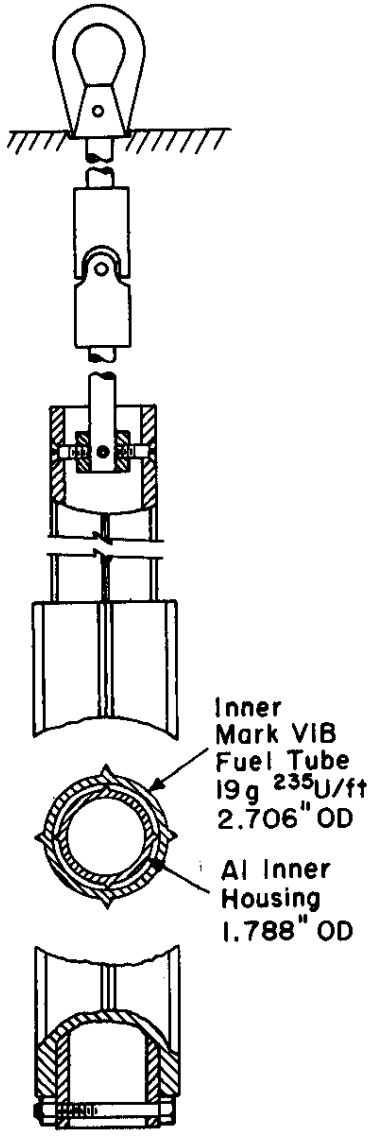

FIG. 8 SE FUEL ASSEMBLY-TYPE B

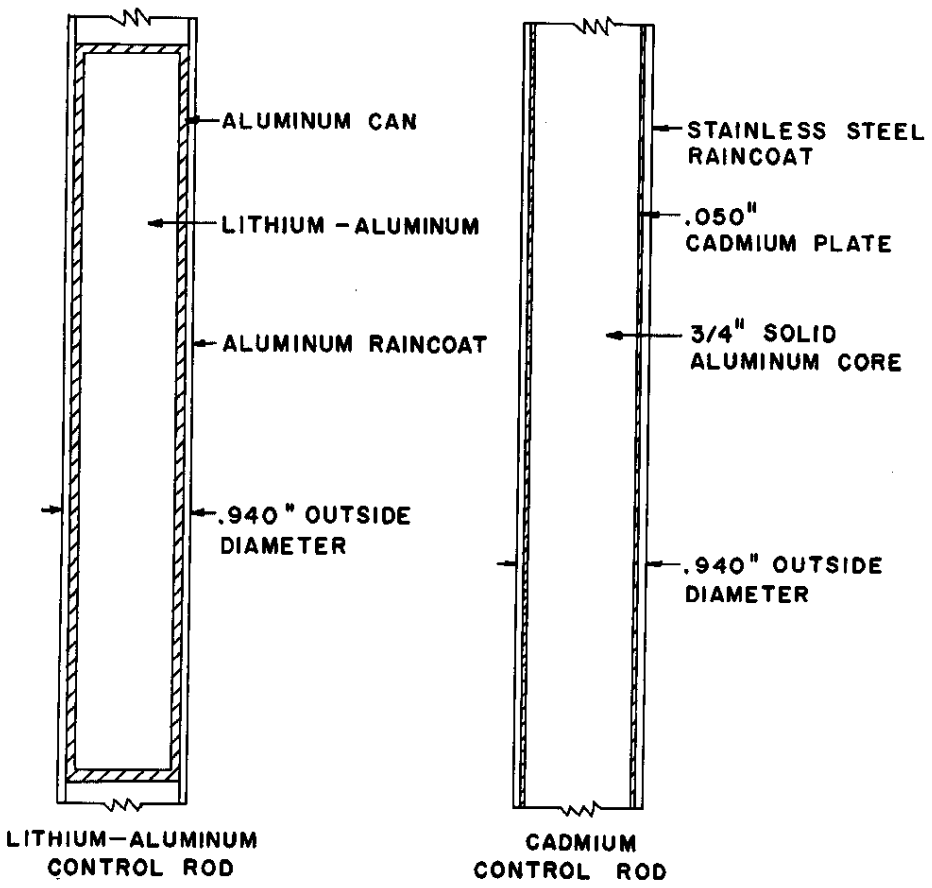

FIG. 9 SE CONTROL ROD DETAILS

Buckling Measurements

A major objective of the SE experiments was to provide buckling values as a basis for designing the full-scale lattice mockup experiments to be performed in the PDP, since these lattices would necessarily be constructed from fuel and target elements similar to those used in the SE. Bucklings were measured by standard flux mapping techniques,[1] using a least-squares computer program to fit the vertical flux distributions (determined with a traveling monitor) to sinh curves and the radial flux distributions (determined by foil irradiations) to Bessel functions. Results are given in Table I.

Another series of buckling measurements was performed with a stainless steel rod 0.375 inch in diameter inserted inside each fuel assembly to mock up the additional aluminum which would be present in the reference two-tube fuel assembly design. These results are summarized in Table II.

TABLE I

Core Bucklings and Control Rod Worths

SE Mockup of High-Flux Lattice
Fuel Assemblies Contain 20 g ^{235}U/ft and 990 g Al/ft

Lattice Configuration[a]	Lattice Buckling, μB		Control Rod Worth, μB
	Uncorrected	Corrected to a Flat Radial Flux	
FZ-0 rod	1505[b]	1503	-
FZ-1 rod	1207	1222	281
1- 3.5% Li-Al control rod			
FZ-3 rod	674	716	787
2- Cd control rods 1- 3.5% Li-Al control rod			
FZ-5 rod	489	541	962
2- Cd control rods 3- 3.5% Li-Al control rods			
FZ-7 rod	374	432	1071
4- Cd control rods 3- 3.5% Li-Al control rods			

(a) See Figure 9 for control rod descriptions.
(b) Due to its high reactivity, this lattice configuration could not be run in the SE. The listed buckling value was obtained by using control rod worth ratios measured for similar lattices in earlier programs.

TABLE II

Worth of 0.375-inch-Diameter Stainless Steel
Rods in Fuel Assemblies of SE High-Flux Mockup

Lattice Configuration	Lattice Buckling, μB	Stainless Steel Rod Worth, μB
FZ-0 rod	1187	321
FZ-1, 1- 3.5% control rod	874	333

Heat Generation in SE Fuel Mockup as a Function of Control Rod Worth

A second set of experiments conducted in the SE determined the variation in azimuthal heat generation within the fuel tubes as control rods were withdrawn from the septifoils.

The heat generation, or more properly the neutron flux producing the heat, was measured by placing manganese pins on the outer surfaces of a mockup fuel assembly as shown schematically in Figure 10. The mockup assembly consisted of a single tube with the dimensions of the outer tube of the two-tube assembly of the actual production lattice and with a fuel concentration close to that of the two tubes (20 g ^{235}U/ft). The mockup assembly tests should give a realistic measure for the production outer fuel tube, but should give a conservative overestimate of flux peaking effects for the combined assembly. The manganese pins were 0.5 inch long and 0.062 inch in diameter. The total activation of such pins gives a reasonable estimate of total fission producing flux in ^{235}U.

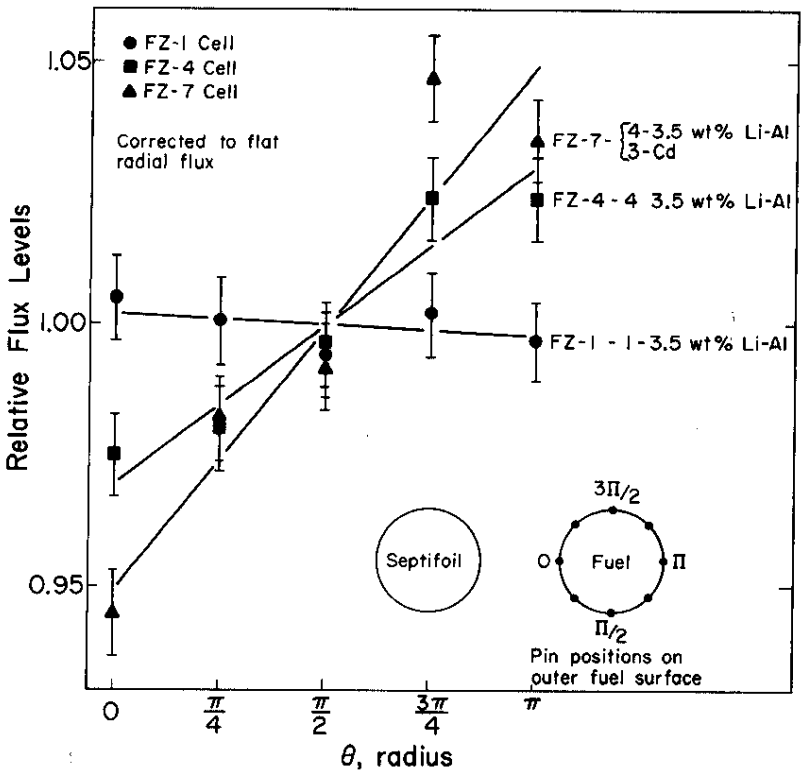

FIG. 10 AZIMUTHAL FLUX VARIATIONS ON FUEL TUBES

The measured pin activations are shown in Figure 10 along with linear fits to the data. The activations are in each case normalized so that the average is unity. The flux variation is seen to be greatest for the heavily loaded septifoils. These flux peaks occur on the side farthest from the septifoil. As rods are removed, the flux variation diminishes until it nearly vanishes for one rod. The no-rod case was not measured because of the high reactivity of this lattice, but it is expected to show a flux peaking in the opposite direction, that is, facing the septifoil. The value of this peaking may be inferred from a plot of flux peaking versus rod worth such as Figure 11. The dashed line extension is obtained by reflecting the linear fit to the data on the $\Phi_{max}/\bar{\Phi} = 1.00$ line. These points were taken from the actual data, not smoothed out curves.

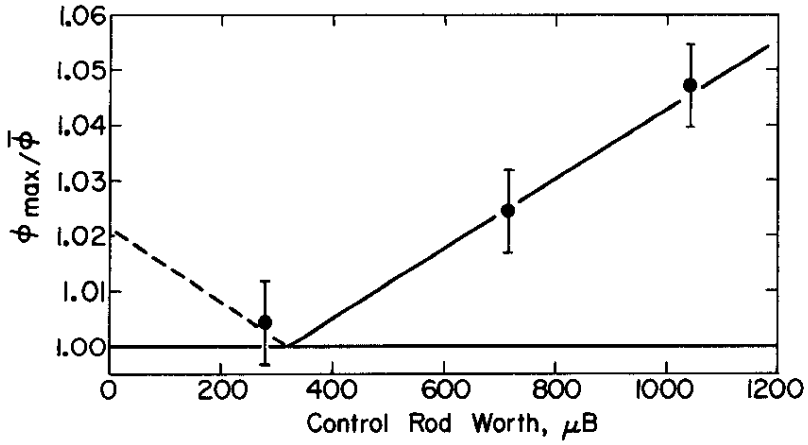

FIG. 11 FLUX PEAKING IN FUEL vs CONTROL ROD WORTH IN SEPTIFOIL

SE Temperature Coefficient Measurements

The temperature coefficient for uniform heating of both the FZ-1 and FZ-7 rod lattice configurations in the SE was measured to be -2.2 $\mu B/^{\circ}C$. This value was determined from vertical flux measurements only, but has been corrected for a calculated change in radial buckling, ΔB_r^2, of 6 μB in heating the SE from 20 to 90°C. The temperature coefficient plots are shown in Figure 12.

A series of experiments was then carried out to demonstrate that a large portion of the measured coefficient results from a change in relative absorptions between the control rods and the fuel assemblies. In one set of experiments, copper strips were attached in intimate contact with the exterior surface of the fuel tubes. Two cases were investigated, both without control

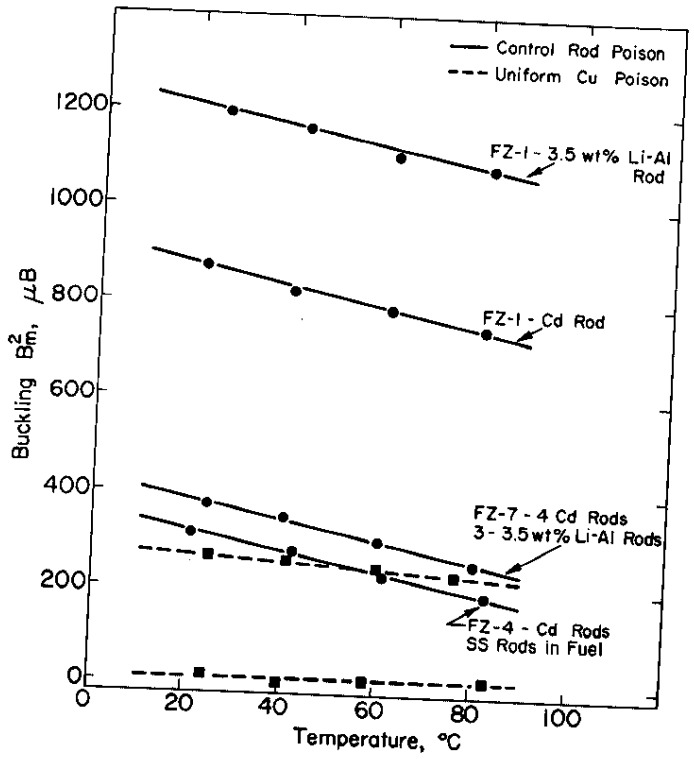

FIG. 12 TEMPERATURE COEFFICIENT AS A FUNCTION OF CONTROL ROD WORTH

rods. In one, the amount of copper added was adjusted to get a room temperature lattice buckling of about 300 μB, equivalent to the lattice buckling when the control clusters each contained four cadmium control rods. In the other, still more copper was added until the lattice buckling was about 0 μB. At zero buckling the effects of leakage are eliminated and the entire coefficient depends on changes in k_∞ with temperature. Figure 12 compares the measured temperature effects in these cases with the effects measured in the configurations with control rods. It is seen that the temperature coefficient is only about one-third as large when the lattice is poisoned down to 300 μB with the copper strips on the fuel tubes rather than with cadmium control rods. This is as expected, because the presence of the copper adjacent to the fuel tube minimizes temperature-dependent changes of the relative flux between the fuel and the poison absorber. No change in buckling with temperature occurred in the lattice poisoned to ~0 μB with copper, indicating no change in k_∞ of this lattice with temperature.

Another set of experiments determined the change in activation ratio of manganese pins between the control rod positions and the fuel positions when the temperature of the moderator was changed.

In order to avoid complications with black absorbers, these measurements were carried out in a lattice containing lithium-aluminum control rods rather than cadmium control rods. Auxiliary measurements showed that the lattice buckling change with temperature was the same with lithium-aluminum control rods as with cadmium control rods when the rod worths were the same (Figure 12). The activation measurements were made with manganese pins placed around the fuel tube and in diametrical holes through the lithium-aluminum control rods. Measurements were made at 20 and 80°C, and exact geometry was maintained, including the use of the identical pins in the identical positions in order to cancel out as many uncertainties as possible. The ratio of the activation of the pins in the control rods to the activation of the pins around the fuel tube increased about 5% when the lattice was heated from 20 to 80°C. This experiment thus confirmed that the change in flux in the control positions relative to the fuel positions makes a significant negative contribution to the moderator temperature coefficient.

MOCKUP LATTICE MEASUREMENTS IN THE PDP

A nuclear mockup of the complete high-flux reactor loading was installed in the PDP.[2] A face map of the mockup loading is shown in Figure 2, and the PDP with its chief auxiliaries is illustrated in Figure 13.

The basic core loading consisted of 108 fuel assemblies, 6 sparjet* tubes, and 19 control assemblies in the central region of the reactor. A hexagonal ring of 18 additional control clusters surrounded the core. The fuel pieces were fabricated from components that were readily available and were similar to those described for the SE in the previous sections. Seven different types of assemblies were used. In every assembly, however, the ^{235}U content (in the form of oralloy-aluminum alloy) was between 19 and 24 grams per linear foot, and in the majority it averaged 20 grams per foot. The cross-sectional area of each assembly was equivalent to about 3 in^2 (aluminum). To reduce the overall reactivity of the lattice and to balance out differences in aluminum content, 1/4- and 3/8-inch-diameter stainless steel rods were selectively added to the less bulky assemblies. Table III gives the ^{235}U, aluminum, and stainless steel content of the seven types of fuel. Figure 14 shows a typical fuel assembly.

* The sparjet tubes serve the double function of injecting jets of cold D_2O into the moderator to ensure desired moderator circulation, and of providing inlets for a liquid neutron poison which serves as a supplementary safety system.

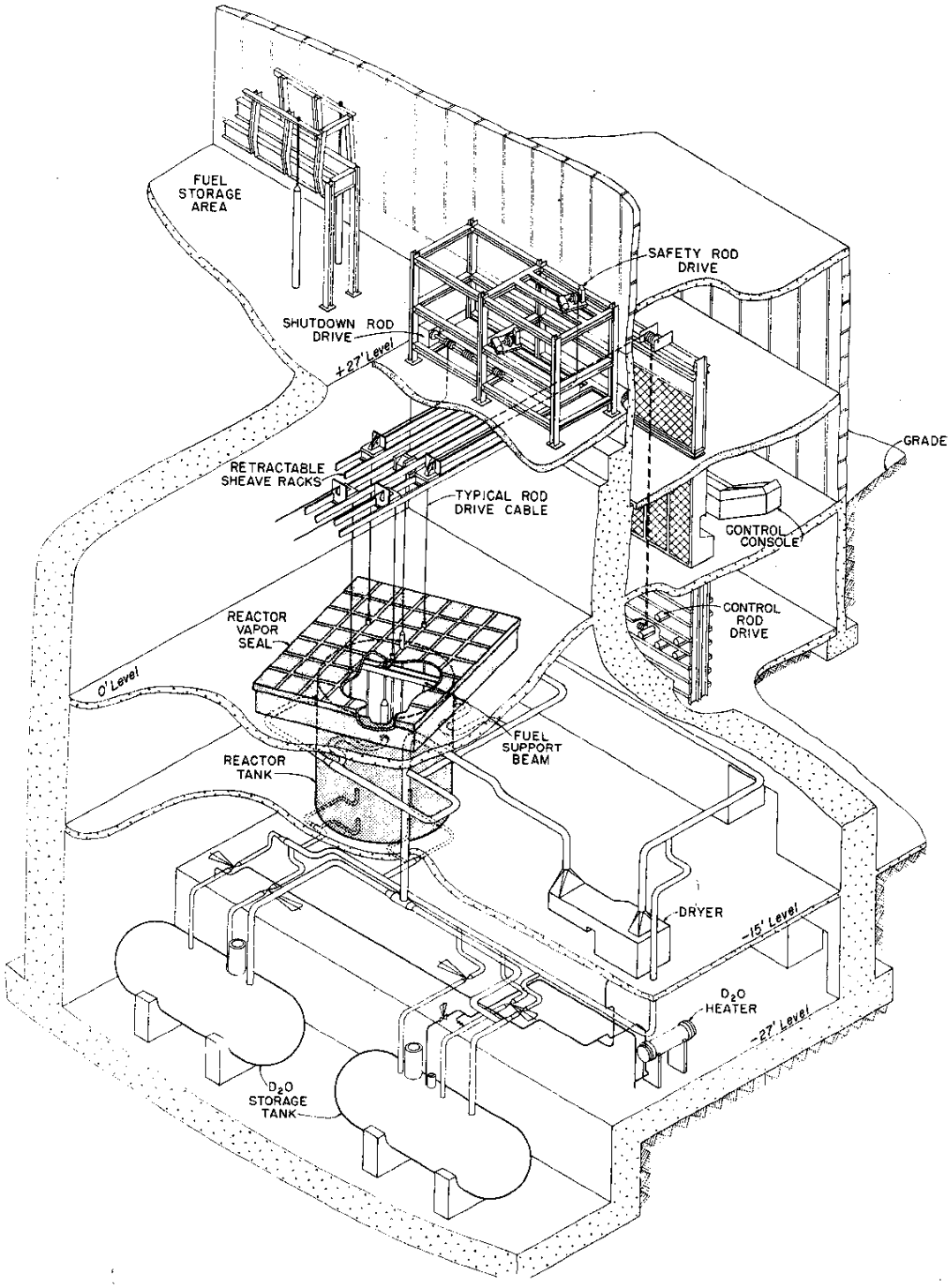

FIG. 13 PROCESS DEVELOPMENT PILE

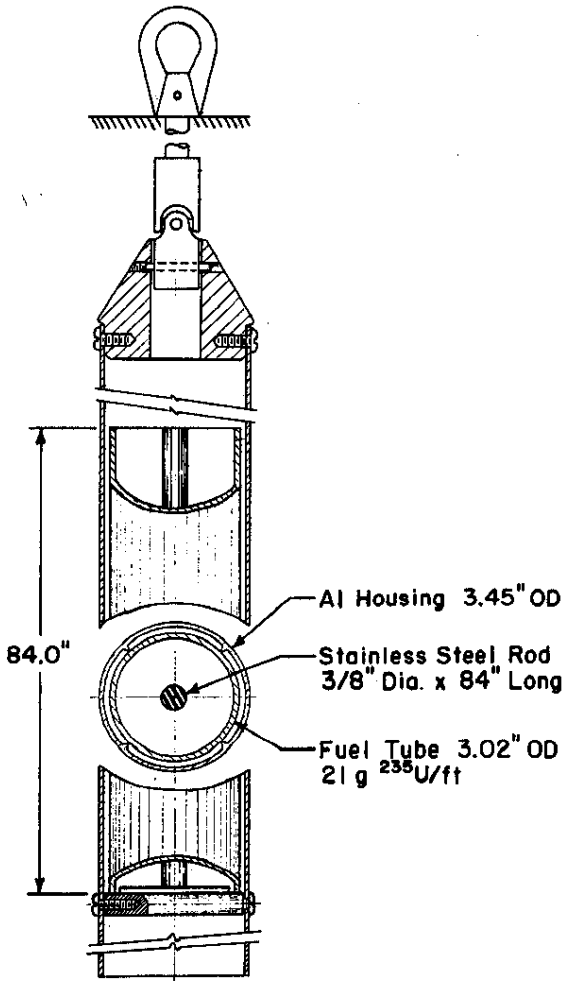

FIG. 14 TYPICAL PDP FUEL ASSEMBLY (HIGH-FLUX MOCKUP)

TABLE III

Fuel Assemblies Used in PDP Mockup of High-Flux Lattice

Type	No. of Assemblies	Fuel Tubes No.	Fuel Tubes g/ft ^{235}U	Cross-Sectional Area, in^2 (aluminum equiv.) Al	SS, Approx	Total
1	24	1	21	2.13	1.0	3.1
2	24	1	19	1.91	1.0	2.9
3	6	2	11,9	3.45	0	3.4
4	31	2	11,9	3.1	0	3.1
5	2	2	11,9	2.8	0.5	3.3
6	8	1	19-25	1.8	1.5	3.3
7	13	1	19-25	1.5	1.5	3.0

The active portion of the fuel was 213 cm long (about 30 cm longer than the planned production reactor loading) and was suspended 55 cm above the PDP tank bottom. The aluminum content above and below the active core was approximately that expected for the operating reactor. The fuel assemblies were located in the lattice in such a way as to give a uniform fuel concentration in each hex. The assemblies that diverged appreciably from 20 g/ft and 3 in^2 aluminum were located in the outer, low-statistical-weight regions of the core to keep the effective perturbations to a minimum.

The six mockups of the sparjet tubes consisted of heavy aluminum tubes with cross-sectional area equivalent to the production lattice assemblies. Control rods in the initial experiments consisted of 0.86-inch-diameter cadmium and 3.5 wt % Li-Al rods. Mockups of the smaller diameter cadmium rods planned for the high-flux load were used in the central hex loadings only.

Two different types of experiments were performed with the PDP mockup lattice. Critical water height measurements with the water level in the range of the active core were used primarily for component evaluations in the central hex. Critical and subcritical measurements at full water heights, with an upper reflector, were used to determine properties of the reactor as a whole. As a basis for these two types of measurements, the initial critical runs determined the uniform control rod complements in the septifoils required to achieve criticality for these two types of measurements, i.e., (a) with the D_2O level 10 to 40 cm below the top of the fuel, and (b) with the moderator level about 100 cm above the top of the fuel. These rod settings are given in Table IV.

Specification of High-Flux Fuel Composition

Early calculations indicated that the ^{235}U concentration in the high-flux fuel assemblies should be about 25 g ^{235}U/ft in order to achieve the desired margin of control* and fuel cycle length with the smaller diameter cadmium control rods. To provide a closer estimate of fuel composition for fuel fabrication purposes, measurements were made in the PDP mockup load to determine the fuel concentrations and control rod configurations for the production lattice which would give bucklings equivalent to those of the mockup loading at criticality. The advantage of this technique is that such quantities as reflector savings and sparjet

* Margin of control (abbreviated MOC) is defined as the degree of subcriticality, expressed in terms of buckling, when all the control rods are fully inserted.

TABLE IV

Critical Control Rod Settings in PDP High-Flux Mockup(a)

Moderator Height, cm	Control Rod Settings(b) Gangs I and II(c) Core	Gang III Reflector	Central Septifoil
300	B,E,F	B,E,F	D at 50 cm
237	B,E,F	B,E,F	0
366	B,E,F(d)	7 rods	A,D,E,F; C at 65 cm

(a) Rod A - Cadmium
B - Cadmium
C - 3.5% Li-Al
D - Cadmium
E - 3.5% Li-Al
F - 3.5% Li-Al
G - Cadmium
Conventional septifoil lettering sequence (see Figure 4)

(b) Indicated rods fully inserted into septifoils unless otherwise stated

(c) Except central septifoil

(d) Rod B in this run only was changed to a 3.5% Li-Al rod

worth are included in the measurement of the mockup loading and do not contribute added uncertainties. In these measurements, two different sets of high-flux fuel assemblies with the exact production dimensions but with different ^{235}U concentrations were substituted into the central hex (6 fuel positions) of the high-flux mockup lattice with the septifoils other than the central one adjusted for criticality at full water height. Control rods in the central septifoil were then adjusted for the reactor to reach criticality at full moderator height. The buckling worth of the rods that had to be withdrawn provided a measure of the MOC for the particular fuel concentration present in the central hex. By extrapolating measurements at two or more fuel concentrations, the fuel concentration for any desired MOC could be specified with reasonable accuracy so long as the desired MOC was in the vicinity of the measured points.

In order to match the mockup lattice core, the test fuel assemblies were 7 feet long instead of the 6 feet required for the production reactor high-flux core. Dimensions of the assemblies are given in Table V. The two fuel sets had average ^{235}U contents of 21.7 and 25.1 g ^{235}U/ft. These were determined by the NTG[4] measurements described in Table VI.

TABLE V

Test Fuel Assemblies - Fuel Specification
Experiments in High-Flux Mockup Lattice

	Dimensions, inches[a]		
	OD	ID	Wall
Outer housing tube	3.420	3.300	0.060
Outer fuel tube, clad	3.020	2.736	0.142
Inner fuel tube, clad	2.354	2.648	0.153
Inner housing tube	1.740	1.640	0.050

Fuel tube lengths 84 inches
Fuel cladding 0.030 inch thick, outer surface
0.020 inch thick, inner surface

(a) See Figure 3.

Several corrections to the PDP measurements were necessary in order to exactly match the conditions of the production loading. These corrections are discussed in the following paragraphs and are tabulated in Table VII.

As discussed in the next section, several control rod complements were considered for the high-flux charges. The control rod set that was chosen for actual use (identical in worth to set No. 2 in Table VIII) was not the same set that was used in the fuel specification measurements (set No. 1). The measured "PDP margin of control" must be corrected by the difference in reactivity worth between the two septifoil loadings. This correction is given in items 1, 2, and 3 of Table VII. Because MOC is determined at startup when control rods are uniformly distributed across the core, the control rod worths in Column C of Table VIII were used in determining these corrections.

The measured worth of the rods that were withdrawn from the central septifoil from the "all rods in" condition to criticality (PDP MOC) is given for each test fuel case in item 4 of Table VII.

The moderator purity in the PDP mockup was 99.45 mol % D_2O while that in the high-flux charges was nominally placed at 99.8 mol %. The corresponding buckling difference amounts to 26 μB.

To permit criticality at a high moderator level in the PDP mockup lattice, additional poison rods were added to outer regions of the core. These rods would not be present in the high-flux charge, and their removal from the PDP mockup would have reduced the measured MOC by 47 μB in each case.

The PDP mockup core was 7 feet long instead of 6 feet as proposed for the high-flux charges. Correcting for this difference added 31 μB to the measured MOC.

TABLE VI

Test Fuel Used in PDP High-Flux Mockup
Measurements to Specify Fuel Composition

	Position in Central hex	Inner NTG[a] Reading	Inner ^{235}U, g/ft	Outer NTG[a] Reading	Outer ^{235}U, g/ft
Nominal 25 g/ft	1	2.56	11.5	3.01	13.2
	2	2.80	12.4	3.01	13.2
	3	2.56	11.5	3.05	13.4
	4	2.57	11.5	3.05	13.4
	5	2.80	12.4	3.05	13.4
	6	2.57	11.5	3.05	13.4
		Avg	11.8	Avg	13.3
		Avg inner and outer = 25.1 g ^{235}U/ft			
Nominal 21 g/ft	1	10.68	10.4	11.1	10.5
	2	9.06	9.8	12.4	11.0
	3	11.48	10.7	11.9	10.8
	4 - 1'[b]	11.82	10.8	11.3	10.6
	4 - 6'	15.64	12.3	11.2	10.6
	5 - 1'[b]	11.48	10.7	11.9	10.8
	5 - 6'	15.64	12.3	11.2	10.6
	6	11.82	10.8	11.3	10.6
		Avg	11.0	Avg	10.7
		Avg inner and outer = 21.7 g ^{235}U/ft			

NTG Standards

Used with Nominal 25 g/ft Fuel: NTG Standard Tube No.	NTG Reading	^{235}U, g/ft	Used with Nominal 21 g/ft Fuel: NTG Standard Tube No.	NTG Reading	^{235}U, g/ft
1655-2	2.17	9.9	1655-2	9.5	9.9
1683-2	2.30	10.5	1683-2	11.0	10.5
1651-1	4.61	19.3	0009-2	30.4	17.6
1604-2	5.09	21.1	1604-2	38.7	21.1
0005-2	8.01	30.9	0005-2	65.9	30.9
			0003-1	73.4	33.2
			0002-2	97.8	41.4

(a) NTG (Nuclear Test Gauge) readings on the two sets were made at different times, using different standards. The standards and their readings are listed below.

(b) In these two assemblies, each fuel tube consisted of a 1-ft-long section and a 6-ft section. The two lengths were weighted 0.1 and 0.9, respectively, in reaching the average ^{235}U composition for the set.

TABLE VII

Margin of Control Determined in PDP Mockup of High-Flux Lattice

^{235}U in fuel assemblies	Buckling, μB 21.7 g/ft	Buckling, μB 25.1 g/ft
(1) Worth of full septifoil used in MOC measurements[b]	1091	1091
(2) Worth of full septifoil equivalent in worth to that planned for high-flux charges[c]	965	965
(3) Difference, (2) - (1)	-126	-126
(4) Measured PDP MOC[a]	277	39
(5) D_2O purity correction	-26	-26
(6) Poison rod correction	-47	-47
(7) Fuel length correction	+31	+31
(8) Thimble correction	+10	+10
Net MOC, (3) + (4) + (5) + (6) + (7) + (8)	119	-119

(a) PDP margin of control (MOC) is defined as the reactivity worth, in buckling, of the control rods that must be withdrawn from the "all rods in" condition to achieve criticality in the PDP.
(b) Septifoil rod worth of Column C, Table VIII control rod set No. 1.
(c) Septifoil rod worth of Column C, Table VIII control rod set No. 2, corrected for presence of two three-quarter length control rods.

TABLE VIII

Worth of Control Rod Clusters Using Small-Diameter Cadmium Rods

Rods Withdrawn[a] from Full Septifoil			No. Rods Remaining In	Worth of Rods Withdrawn, μB[b] A Measured	B Corrected to Flat Flux	C Corrected to High-Flux Charge
Set No. 1 - Cd Diameters						
0.25"	0.45"	0.86"				
		D	6	101	96	99
		A,D	5	211	200	207
		A,D,G	4	353	334	346
	E	A,D,G	3	525	498	515
	B,E	A,D,G	2	730	693	715
C	B,E	A,D,G	1	910	863	891
C,F	B,E	A,D,G	0	1114	1057	1091
Set No. 2 - Cd Diameters						
0.25"	0.435"	0.45"				
C,F			5	98	93	96
	D,G		5	152	144	149
C,F	D,G		3	319	303	313
C,F	D,G	A	2	507	481	497
C,F	D,G	E	2	540	512	529
C,F	D,G	A,E	1	790	750	774
B,C,F	D,G	A,E	0	995	944	975

(a) Rod positions in septifoil are designated clockwise A through G with the G position in the center of the septifoil (Figure 4).

(b) These rod worths are for full length rods. Current plans call for two 2/3 length rods to replace two of the full rods. This will decrease the total worth of set No. 2 from 975 to 965 μB (Column C).

The reference FZ-0 buckling for a uniform mixture of assembly types 1 and 2 of Table III but without the added stainless steel is 1505 μB. The reference FZ-0 buckling for the production 22.0 g/ft assemblies is 1460 μB.

The final correction in Table VII accounts for the fact that the mockup lattice in the central hex contained no instrument or safety rod thimbles. Correcting for thimbles that would be present in the actual lattice added about 10 μB to the measured MOC.

A plot of the resulting MOC versus the ^{235}U composition of the test fuel is given in Figure 15. From this plot the fuel composition for the desired MOC of 100 μB was determined to be 22.0 g/ft (the sum of the inner and outer fuel tubes). However, this MOC specification of fuel concentration applies to a demonstration load only. Addition of target rods to the sparjets or replacing fuel assemblies with ^{252}Cf-producing (or other) targets would increase the MOC unless the fuel concentration was increased a corresponding amount.

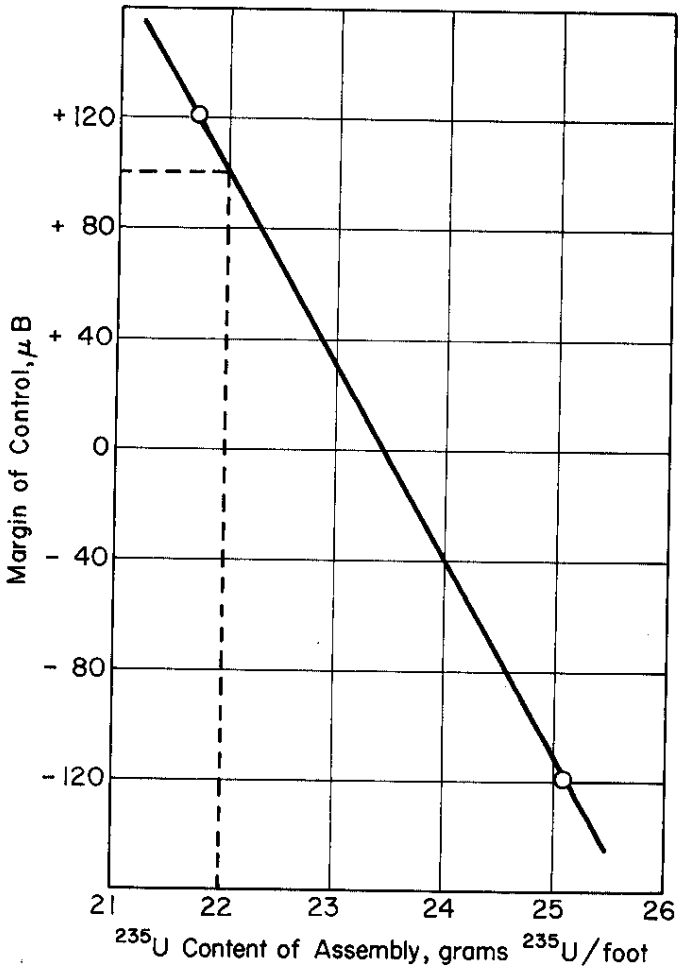

FIG. 15 MARGIN OF CONTROL IN PDP MOCKUP OF HIGH-FLUX LATTICE

Control Rod Experiments

Worths of several combinations of control rods in the control clusters were measured by the central hex technique in the PDP mockup load. Additional control rod worth measurements made in the production load in the PDP will be discussed later in this report.

Because of the complex mixture of fuel assemblies in the mockup lattice, it was impossible to make central hex buckling determinations from geometrical considerations alone. Meaningful measurements could be made, however, by the use of a critical water height calibration curve obtained by inserting lattices with known bucklings into the central hex. For this purpose the known lattice was taken to be the SE high-flux mockup lattice, a one-to-one mixture of fuel types 1 and 2 of Table III, but with no added stainless steel. The calibration buckling values for this lattice are given in Table IX. The calibration rod worths are given as measured and with calculated corrections to a flat radial flux.

TABLE IX

Buckling Values for Calibration Lattice

Lattice Configuration	Rods Withdrawn from Full Septifoil		Worth of Rods Withdrawn, μB (SE measurements)(a)	
	0.86" Cadmium	0.808" 3.5% Li-Al	As Measured	Corrected to Flat Radial Flux
FZ-5 rod	D,G		115	109
FZ-3 rod	D,G	E,F	300	288
FZ-1 rod	A,B,D,G	E,F	833	790
FZ-0 rod	A,B,D,G	C,E,F	1131	1071

(a) Based on reference buckling of 1505 μB for a uniform mixture of fuel assembly types 1 and 2 of Table III.

For the PDP mockup measurements, the control rods consisted of cadmium cores of different diameters contained in solid aluminum sheaths 0.94 inch in diameter. The worths of the combinations tested are given in Table VIII. Column A gives the measured rod worths, column B the rod worths in a flat flux, and column C the rod worths at a time when the control rod settings across the high-flux core are uniform and the Gang III (reflector) septifoils are fully loaded.

The buckling worths of various single control rods were also measured in the PDP center hex. These worths, corrected to a reference flat radial flux, are given in Table X. Because of the very light fuel load, the worth of rods in the safety rod positions is seen to be closely that for the same rods in the septifoils.

TABLE X

SE and PDP Control Rod Worths
and Estimates of Rod Heating

Rod Type	Rod Worth, μB[a] Septifoil	Rod Worth, μB[a] Safety	Minimum Rod Worth as Safety, Δk_{eff}	Rod Reactor Heat, kw/MW[b]
0.86" D Cd, SS Clad	457	448	14.2	15.9
0.625" D Cd, Hollow	390	-	9.7	9.0
0.450" D Cd, Hollow	306	-	-	-
0.250" D Cd, Solid	189	180	6.0	5.5
0.210" D Cd, Solid[c]	-	-	5.0	4.7
14.4S Li-Al	428	-	-	-
3.5% Li-Al	286	-	-	-
1.0% Li-Al	149	-	-	-

(a) Corrected to a flat radial flux.
(b) Rod heat production rates are given as total rod heat production in kw per MW of power in each of the adjacent fuel assemblies. Heat production rates apply to either rod position.
(c) Not measured, estimates are based on extrapolation of other measurements.

Heat production rates for control rods in the operating high-flux lattices were computed from the neutron and gamma ray absorptions. The initial (start of cycle) heat production rates are given in Table X relative to the average power produced in each of the adjacent fuel assemblies. This latter quantity may vary with radial position and with time. Engineering estimates indicate that initial heat production rates of 5 kw per reactor MW for the safety rods and 9 kw per reactor MW for the septifoil rods are in a safe operating range. Thus an accidental insertion of a single 0.625-inch-diameter control rod or of an 0.25- or 0.21-inch-diameter safety rod (which are all expected to be withdrawn during high power operation) would not result in a meltdown of the rod. Heat production rates for the Li-Al rods are not quoted because all exceed the safe limit.

Shutdown reactivity worths of the cadmium safety rods were computed from the measured bucklings, and the results are also given in Table X. The computations assumed one rod per hex over the 19-hex core. The quoted minimum worths were obtained for initial startup conditions with fresh fuel, cold moderator, and fully loaded septifoils in the reflector. The results indicate that safety rods as small as 0.21-inch diameter can be used to give the desired 5% minimum reactivity worth.

Additional safety rod worth measurements using actual production safety rods were made in the production fuel charge in the PDP. These measurements are discussed in a later section.

Because of the excessive heat production in conventional Li-Al control rods, the high-flux operation required control rods with lower heat production rates such as the small diameter cadmium rods (or other rods in which the absorber emits gamma rather than alpha rays on neutron capture). However, in order to best utilize the large amount of production operating experience with different combinations of Li-Al control rods, it was convenient to have a defining relation giving the diameter of a cadmium rod equivalent to any given strength of Li-Al control rod. Rods which are equivalent on an individual basis may then be assumed to be equivalent in the combinations encountered in normal control rod clusters. The measured rod worths used in obtaining this defining relation are listed in Table XI.

TABLE XI

Individual Control Rod Worth Comparison

Cd Rod Diameter, inch	Li-Al Rod(a)	Rod Worth, μB(b)
0.860	-	457
-	14.4S	428
0.625	-	390
0.450	-	306
-	3.5%	288
0.250	-	189
-	1%	149

(a) % denotes wt % natural Li.
S denotes ratio of ^6Li atoms to those in same volume of 1 wt % natural Li rod.
(b) Corrected to a flat radial flux.

All control rods considered had an overall diameter of 0.940 inch. The Li-Al rods had an active core of 0.808 inch and were clad with aluminum. The cadmium rods were also clad with aluminum except for the 0.860-inch rods, which were stainless steel clad. Calculations using various models were also made and checked by comparisons with the PDP central hex experimental data.

Equivalent rod worths derived from these measurements are shown in Figure 16. The corresponding calculated values are shown by the curves. The smooth curves represent "Blackness Theory" calculations. The upper smooth curve assumed monoenergetic neutrons with energies given by the most probable velocity of neutrons in equilibrium with the moderator. The lower smooth curve was based on the same theory except that a numerical integral over the Maxwellian distribution was used along with an assumed spectrum hardening (based on survey THERMOS[5] calculations) at the surface of the Li-Al rod. The latter calculations are seen to be in good agreement with experiment and with direct THERMOS calculations over a shorter range given by the dashed curve of Figure 16.

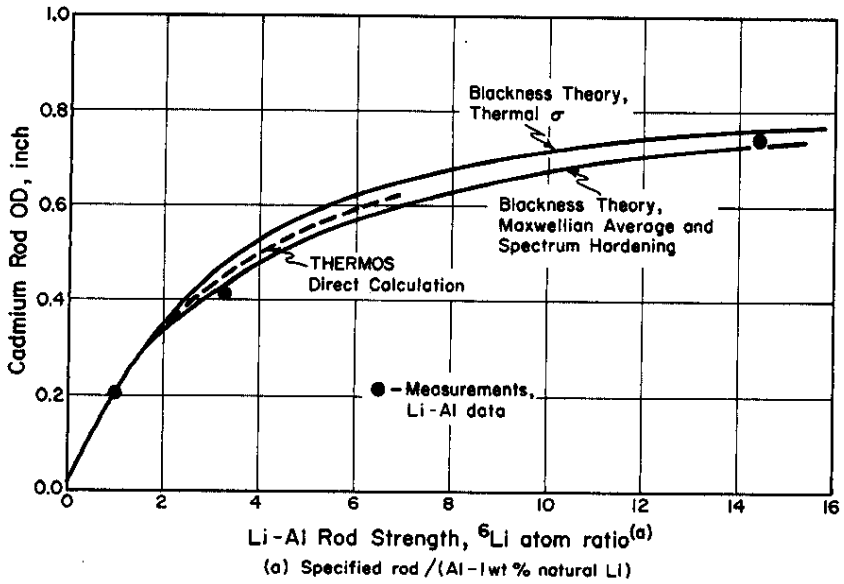

FIG. 16 COMPARISON OF SMALL-DIAMETER CADMIUM RODS WITH Li-Al CONTROL RODS IN THE HIGH-FLUX LATTICE

Prompt Temperature Coefficient

The prompt temperature coefficient* was measured for high-flux lattice fuel assemblies of 25 g ^{235}U/ft concentration. Air-filled insulating cans of aluminum, 3.780 inches in OD and 0.060 inch in wall thickness, were inserted around the 25 g/ft test assemblies in the center hex of the PDP. Hot (~80°C) and cold (~25°C) D_2O was circulated alternately through the three coolant channels surrounding the fuel tubes, while the pile was kept exactly critical with a pair of control rods which had been calibrated

* The prompt temperature coefficient is that portion of the overall temperature coefficient of reactivity associated with the fuel assembly itself.

in terms of center hex buckling. Temperatures were monitored by thermocouples in the inlet and outlet channels of the test assemblies. The temperature coefficient was thus determined as a change in buckling of the test assembly lattice per unit temperature change. Coefficients were measured for FZ-0 and FZ-3 lattice configurations; the FZ-3 configuration used three cadmium rods of 0.86-inch diameter and corresponded roughly to a full septifoil of the smaller diameter cadmium rods scheduled for the high-flux lattice. The experimental results are given in Table XII. These coefficients are safely negative and from the standpoint of the prompt temperature coefficient, the high-flux charge can be operated safely.

TABLE XII

Prompt Temperature Coefficients in the High-Flux Lattice

No. of Measurements	Lattice Configuration	Prompt Temp Coeff, $\mu B/^{o}C$
3	FZ-0	-0.33 ±0.03
2	FZ-3	-0.30 ±0.03

Flux Transient Measurements

It has become standard practice to measure prompt temperature coefficients under actual operating conditions in the production reactors as well as in the zero-power mockups. The production measurements depend on analyses of the flux transient resulting from step reactivity changes produced by special "Δk rods." However, in order to derive prompt temperature coefficients of reactivity from reactor transient analyses, it is necessary to have detailed knowledge of system parameters on the one hand and of flux perturbation effects and the delayed neutron behavior on the other. Failure to know all these quantities precisely may lead to uncertainties in the interpretation of the measurements. In order to supply such information for the high-flux reactor loading, Δk rod experiments were performed in the PDP mockup employing, as far as possible, the identical equipment used for the operating reactors.

The PDP loading for this experiment is shown in Figure 2. A single, standard Δk rod (a shutter-connected arrangement of telescoping cadmium sections) was placed at the center of the lattice replacing the central control cluster. Three Δk rods are normally used in the production measurements, but because of the reduced pile size and the large migration area of the high-flux load, even a single conventional Δk rod would give a too large

reactivity change in this load. For the PDP experiments, the reactivity change was further reduced by shielding the Δk rod with two normal cadmium rods placed on opposite sides of the Δk rod. The worth of the shutter motion was measured at reduced water heights by the critical water height method. This buckling worth, ascribed to the central hex, was 26 μB, approximately one-third that expected for an unshadowed rod.

The kinetic measurements were made at full water height. The added poison required to reach full water height was obtained by inserting the sparjet mockups and by adding a few remote control rods located at scattered radial positions. The expected pile reactivity change, $\rho = 0.00095$, due to the shutter motion in this configuration was computed from the measured buckling, a migration area of 370 cm^2 for the core, and calculated statistical weights.

If in a critical pile a localized reactivity change is made, two effects are normally observed: a new flux shape is established rapidly, and an overall increase or decrease of power level then occurs. To investigate the magnitude of the change in flux shape, a compensated ion chamber was placed alternatively in one of two positions: just outside the central hex at the top level of the core, or at the vertical midplane of the core in the radial reflector near one of the outer septifoils. The results of the experiment are shown in Figure 17. The response for both detector positions is very nearly the same (compare the closed circles and crosses) for the flux levels as indicated on a high-speed strip-chart recorder. This result indicates that, for this location of the Δk rod, the flux shape change is small compared to the overall reactor response. The digitized output on the punched paper tapes (open circles) agrees with the strip-chart data for the decreasing fluxes but disagrees with the increasing fluxes. It is not now known which calibration is most likely to be in error.

The calculations were made by numerical integration of the reactor kinetics equations using an IBM 704 computer. A moderator absorption probability, T_γ, of 0.8 was assumed for γ rays with energies sufficient to give photoneutrons. The experimental data are seen to fit the computed downgoing curve for $\rho = 0.00096$ except at times from zero to 5 seconds. The upgoing fluxes agree less well, both for magnitude and for shape.

The application of the PDP measurements to the interpretation of prompt temperature coefficient measurements is not certain. The discrepancy in the vicinity of one second is of particular importance, since it is this time interval that most sensitively affects the value assigned to the prompt temperature coefficients.

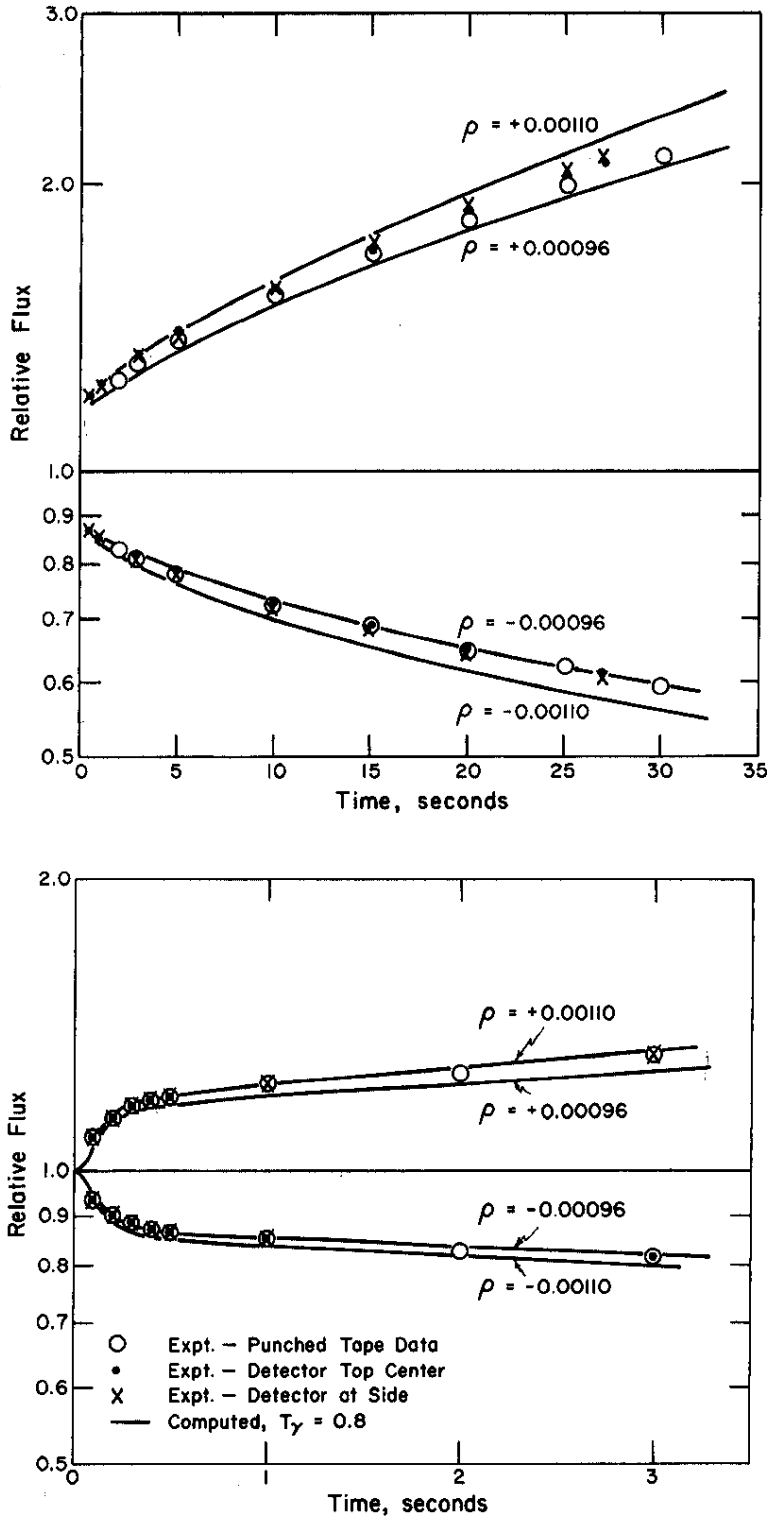

FIG. 17 FLUX TRANSIENT RESPONSE OF PDP MOCKUP LATTICE TO Δk ROD MOTION

Effect of Light Water in Coolant

The effects of adding light water to the fuel assembly coolant channels were determined by measuring the change in critical water height resulting from the addition of light water to the six fuel assemblies in the central hex of the high-flux mockup lattice. Light water was added in two steps: the first taking the coolant isotopic purity from 99.5 mol % D_2O to 58%, and the second taking the purity to 100 mol % H_2O. The results are given in Table XIII.

TABLE XIII

Buckling Change Resulting from Light Water Addition to Fuel Assemblies in PDP Mockup

Mol % D_2O in Test Assemblies	Vertical Buckling Change, μB	Average ΔB_m^2/% H_2O, μB
99.46	-	-
58	-35	-9.9
0	-126	-11.9

The tabulated results are not strictly applicable to the production operating conditions inasmuch as the structural details of the test assemblies required that all of the coolant inside the assembly be uniformly mixed. Hence the coolant coefficient observed in these measurements is larger than would be obtained in operating fuel assembly because, for any conceivable method of light water addition in the production loading, the central cavity of the fuel assembly, which has a very low coolant flow rate, would not be affected until after the light water had poisoned the bulk moderator. These measurements do show, however, that the coefficient is safely negative as predicted by calculations.

Flux Monitoring Instrumentation Response

The thick radial reflector and the outer (Gang III) septifoils in the high-flux charge are expected to suppress the startup neutron flux in the shield, where the startup flux detecting instruments are located, to values much lower than those in normal production charges. Further, it is expected that rod motions in the Gang III septifoils will result in instrument response that is not representative of the actual pile power; i.e., pulling rods from Gang III will "unshield" the core from the instruments, giving a large instrument response even though the actual pile power increase may be quite small. To determine the magnitude of these effects, indium foil irradiations were made in the high-flux mockup lattice with three different control rod loads in Gang III septifoils. The indium foils were irradiated

at the locations shown in Figure 18. The results, in terms of relative thermal neutron flux, are given in Table XIV.

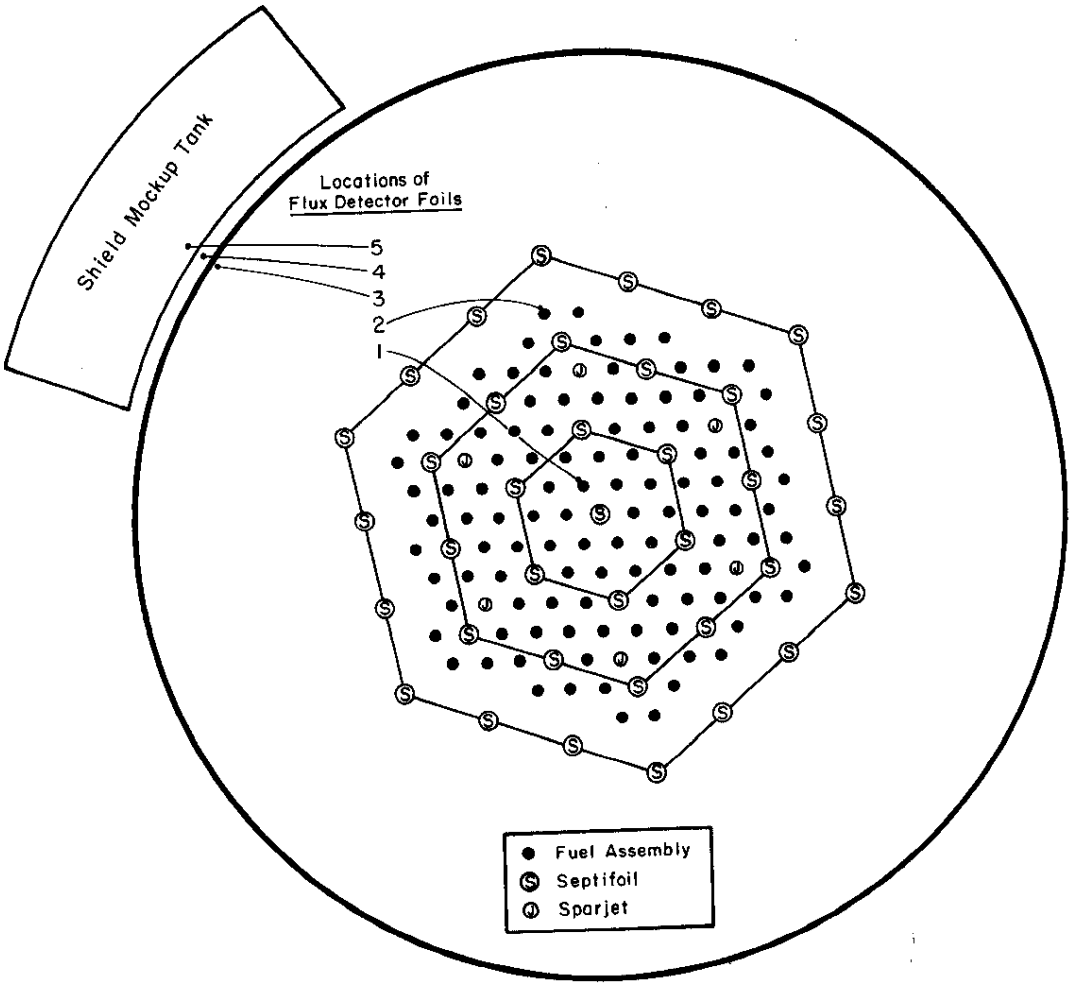

FIG. 18 FOIL LOCATIONS FOR STARTUP INSTRUMENT RESPONSE TESTS IN PDP MOCKUP

TABLE XIV

Neutron Flux in High-Flux Mockup

Foil Location (Figure 18)	Relative Flux Number of Control Rods in Gang III Septifoils 7	2	0
1. Fuel in central hex	1.0	1.0	1.0
2. Fuel at edge of core	0.24	0.28	0.38
3. Edge of moderator	0.0013	0.0026	0.0056
4. Outside of tank	0.00036	0.00059	0.0014
5. Within shield wall	0.00011	0.00023	0.00046

Comparison of the results in Table XIV with results from other production charges reveals that the flux at the instruments is much lower in the high-flux charge. In addition, Table XIV shows that withdrawing seven rods from the Gang III septifoils would result in an instrument reading increase of a factor of 4 at constant pile power.

The implication of these results is that in-pile flux measuring instruments are required during fuel loading operations and during initial startup, and that Gang III rod manipulations will require unusual operating care.

In an additional subcritical experiment, a neutron source was moved to various locations through the high-flux mockup core and instrument readings at the outside edge of the reactor tank were recorded. These measurements indicated that the present production reactor source elevation, coincidentally near the top of the high flux core, gives twice the instrument response, at subcritical, that would be obtained if the source were lowered to the center of the core.

D_2O Moderator Purity Coefficient

The moderator purity coefficient of reactivity was found to be about 100 μB/mol % D_2O in the measurements in the SE. Additional measurements were made in the PDP mockup lattice to confirm this result. The moderator purity in the PDP was raised from 99.440 mol % D_2O to 99.487 mol % D_2O by the exchange of 27,000 lb of D_2O for specification D_2O (99.75 mol %). Critical moderator heights were measured before and after the D_2O exchange at three different critical rod settings in the central septifoil. The measured coefficient, 98 μB/mol % D_2O, agrees very well with the SE result. The details are given in Table XV.

Target Assembly Buckling Worth

The original high-flux lattice design called for three target assemblies replacing three fuel assemblies just outside the central hex. Each assembly was to contain 150 g of ^{242}Pu in four 2-foot-long, 1-inch-diameter columns, centered vertically in the high-flux core. These assemblies were mocked up using 1-inch-diameter aluminum rods 2 feet long centered in the mockup core. The locations of the three assemblies are shown as positions 1 in Figure 19. Critical moderator height measurements with the three targets in place and with the usual fuel replacing the targets were made with two different control rod settings in the central septifoil. The average buckling decrease on replacing the three fuel assemblies with the target mockups was 85 μB.

TABLE XV

Moderator Purity Coefficient of Reactivity

Rod in Central Septifoil	B_z^2(a) at 99.440 mol %, μB	B_z^2(a) at 99.487 mol %, μB	ΔB_z^2, μB
0.86 inch Cd	234.15	238.55	4.40
0.625 inch Cd	245.27	249.23	4.46
None	327.10	332.04	4.94
		Avg	4.60

D_2O change = 0.047 mol %

Coefficient of reactivity = 4.6/0.047

= 98 μB/mol % H_2O

(a) Number of significant figures corresponds to precision in measuring water heights (relative) and not to knowledge of absolute bucklings.

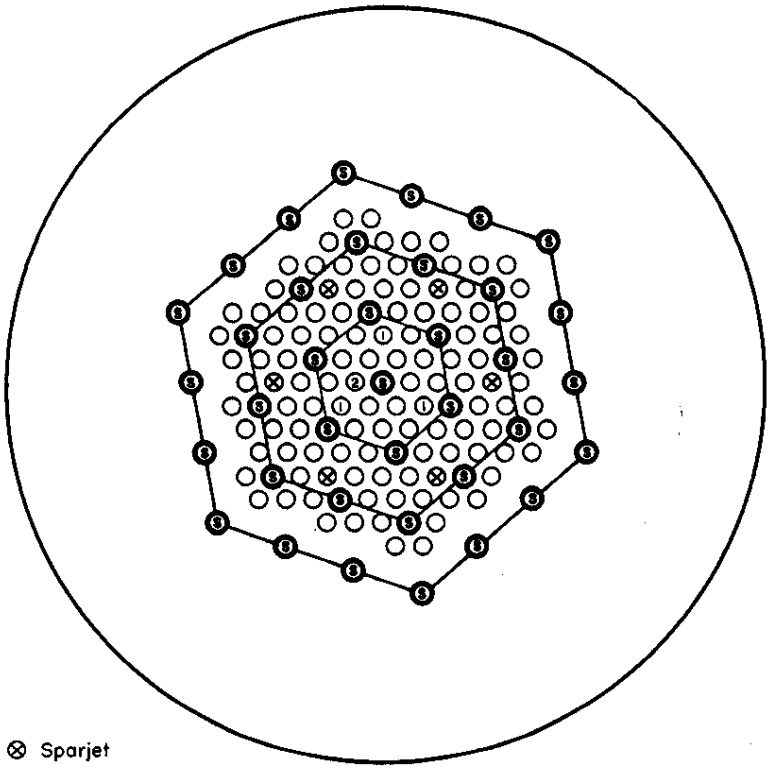

⊗ Sparjet
Ⓢ Septifoil
○ Fuel Assembly
① Positions of Targets in Exp 1
② Positions of Targets in Exp 2

FIG. 19 TARGET LOCATIONS FOR PDP MOCKUP TESTS

Gang III Control Rod Worths

The worth of control rods in the outer ring of septifoils (Gang III) was measured at three critical moderator heights. The results, given in detail in Table XVI, show that a seven-rod loading of all Gang III septifoils is worth 82 μB.

TABLE XVI

Gang III Control Rod Worths

Rods in Gang III	B_z^2, μB	ΔB_z^2 from Zero Rod Case, μB
7 (0.86" Cd A,B,D,G 3.5% Li C,E,F)	182	82
2 (0.86" Cd - B 3.5% Li - E)	213	61
None	274	-

Sparjet Worth

In the course of running other experiments in the mockup lattice, the reactivity effect of replacing the six sparjets with mockup fuel assemblies was obtained. It was 63 μB. Table XVII gives the details.

TABLE XVII

Sparjet Worth

Sparjet Positions Contain	B_z^2, μB	ΔB_z^2 from Sparjets in, μB
Sparjets	327	-
Tubular mockup fuel	390	63

D_2O Moderator Temperature Coefficient

The moderator temperature coefficient of reactivity was measured in the mockup lattice in the PDP. Similar measurements from the SE were described in an earlier section. However, the SE measurements applied only to the lattice core and could not take into account the effect of the large D_2O reflectors. The

reflectors were expected to produce a positive contribution to the coefficient.

The overall temperature coefficient was measured with two different control rod configurations in the PDP. In one, the outer ring of septifoils (Gang III) was emptied of control rods, thus giving full play to the radial D_2O reflector. In the other, the Gang III septifoils each contained three control rods, thus partially reducing the effectiveness of the reflector. Criticality measurements were taken for both lattice configurations, first at 18°C and then at 29°C. All measurements were made at full (370 cm) water height, and the buckling difference between the cool and heated conditions was obtained from changes in the critical control rod settings in the central septifoil. The effect of these calibrated control rods on the overall pile was in turn based on calculated statistical weights.

The experimental results are given in the first column of Table XVIII. These results differ appreciably from the -2.2 μB/°C measured in the SE. However, the PDP conditions also differed from those in the SE in two important respects: the effect of the reflectors is calculated to be a positive contribution of about +0.2 μB/°C; the PDP fuel assemblies were poisoned down with stainless steel rods while those in the SE were not. Corrections for these effects give a coefficient of -1.8 μB/°C from both facilities. The last column of Table XVIII gives an estimate of the temperature coefficient which would actually be observed in the production reactors.

TABLE XVIII

Moderator Temperature Coefficient in High-Flux Mockup Lattice

	Temperature Coefficient, μB/°C		
Lattice Configuration	Overall	Core	Operating Reactor (cool reflector)
PDP			
3 rods in Gang III	-1.6	-1.8	-1.7
No rods in Gang III	-1.5	-1.7	-1.7
SE			
No SS poison		-2.2	
With SS poison		-1.8	

Petaling Experiments and Calculations

As part of a program to reduce the amount of reactivity which could be added to the high-flux lattice by a single control rod driving out of the reactor, it was proposed to operate the lattice with nonuniform control rod loadings in the septifoils. Nonuniform loadings of the Gang II septifoils (outer 12 septifoils in the core) can be expected to lead to flux petaling, i.e., to flux peaks in the outer core regions immediately adjacent to the lighter septifoils. If the petaling becomes sufficiently great, the extra heat production in the fuel in the petaled regions could necessitate reducing the overall power level of the high-flux charge. Accordingly, a short program was carried out in the PDP to determine how much petaling resulted from the removal of full control rods from individual Gang II septifoils. Measurements were also made of the reduction in petaling which could be achieved by adding control rods to the appropriate Gang III septifoils. A companion program of calculations using the computer code PDQ-03[6] was tested against the experiments.

The flux measurements were made by irradiating gold pins in the positions shown in Figure 20. A base distribution was established by performing the irradiation with uniform loadings in all septifoils. Later irradiations were then evaluated as differences from this base case. Table XIX gives the septifoil configurations used in the measurements. The flux petaling is shown in Figures 21 and 22, which plot the percent deviation of the thermal flux in the petaled cases from that in the base case. The plots run counterclockwise over the half pile extending A to AA in Figure 20. The maximum measured increase in flux at the interstitial measurement positions was comparatively small, about 6%. Fuel assemblies immediately adjacent to the lightened septifoils may run slightly higher. As shown by Figure 22, the use of the Gang III septifoils decreases the petaling somewhat but does not eliminate it. However, the problem is not a serious one.

Results of the PDQ calculations are also shown in Figures 21 and 22. While the match to the experiments is not exact, the calculations appear quite adequate for evaluating these small effects and will be used, together with the actual production operating experience, in future petaling studies.

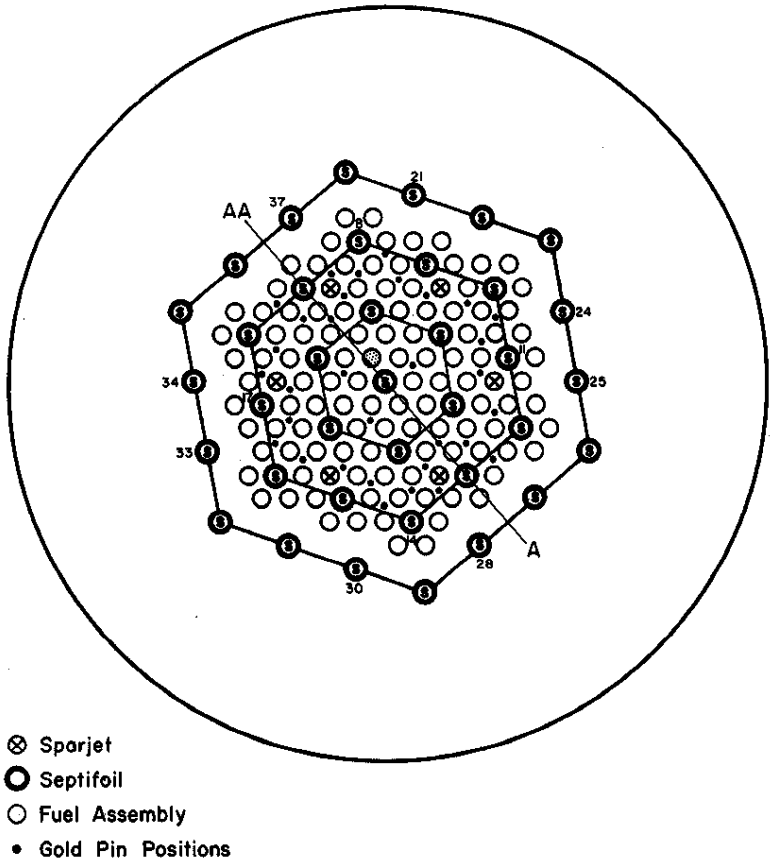

FIG. 20 GOLD PIN LOCATIONS FOR PDP MOCKUP STUDIES OF PETALING

TABLE XIX

Septifoil Rod Loadings for Petaling Studies

Test	Septifoil Rod Loadings		
	Gang I	Gang II	Gang III
1	3 Li-Al rods	3 Li-Al rods in all septifoils	2 Li-Al rods in all septifoils
2	Same as in Test 1	Same as Test 1 except one rod has been removed from septifoils 8, 11, 17, and 14	Same as Test 1
3	Same as Test 1	Same as Test 2	Same as Test 1 except 4 Li-Al rods have been added to septifoils 21, 24, 25, 28, 30, 33, 34, and 37

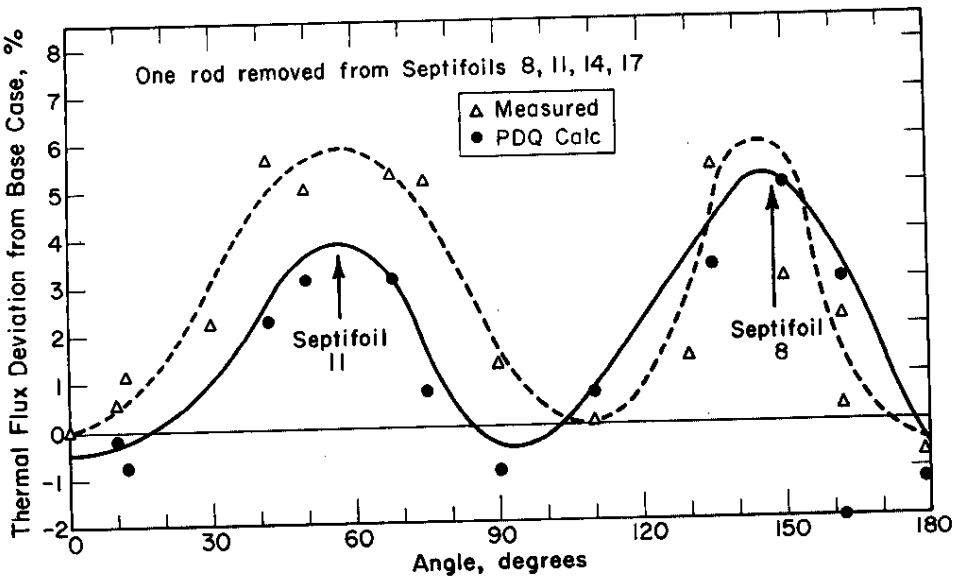

FIG. 21 FLUX PETALING WITH NONUNIFORM SEPTIFOIL LOADINGS IN GANG II

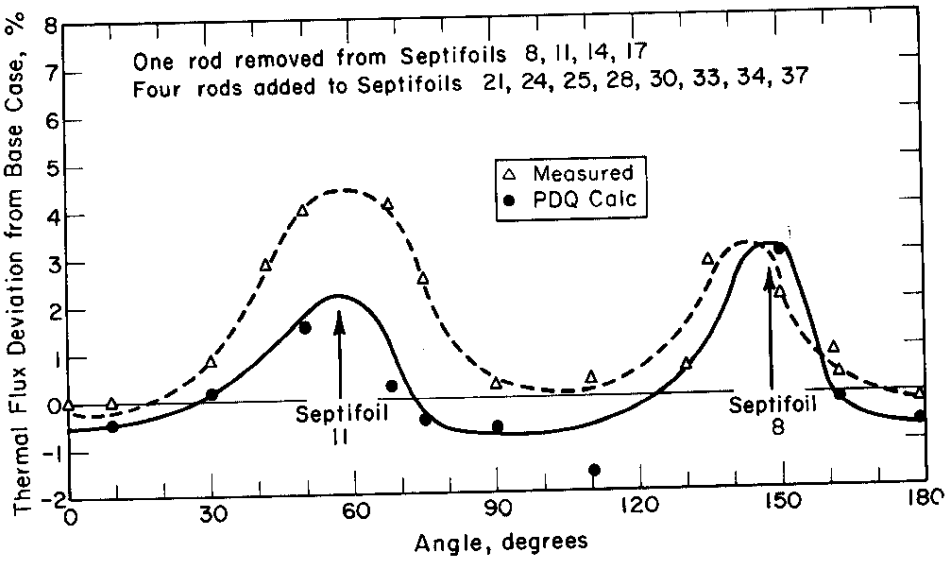

FIG. 22 FLUX PETALING WITH NONUNIFORM SEPTIFOIL LOADINGS IN GANGS II AND III

PDP MEASUREMENTS WITH FULL CHARGE OF PRODUCTION FUEL

Following the experiments with the mockup fuel loading in the PDP, a full charge of high-flux lattice fuel and control rods that were destined for the production reactors was installed in the PDP, and a series of experiments were performed. The primary purpose of the experiments was to obtain a more precise measure of the margin of control that could be expected in the production reactors, but additional parameters were also measured.

Margin of Control Determination

The MOC is defined as the change in lattice buckling resulting from pulling the partial length control rods from their down limits to their initial operating position (~5% withdrawn) and then adjusting the full length rods until criticality is reached. The measured MOC was obtained by analyzing two separate, full-pile, critical runs in the PDP. In each run a preselected number of control rods were first removed from the septifoils in Gangs I and II and then additional control rods were pulled from the center septifoil until criticality was reached. The critical settings are given in Table XX. The known rod worths (measured in earlier studies) and appropriate vertical and radial statistical weighting factors, obtained by assuming a cosine flux shape in the vertical direction and a J_o shape in the radial direction, were used to determine the change in lattice buckling due to the removal of the excess control rods from the pile. This buckling number is the margin of control of the lattice in the PDP. To be applicable to the production charges, the PDP margin of control must be corrected for differences in water purity and in number and position of the targets in the lattice. The change in MOC due to the difference in water purity between the PDP (99.5 mol % D_2O) and the production reactor (99.75 mol % D_2O) is 20 μB.

Making these evaluations for both of the critical configurations of Table XX yields about the same result, namely a predicted MOC of 162 μB for the condition of one target assembly in the central hex (which was the actual condition in the first charge). If the target had not been present the MOC would be 162 - 30 = 132 μB, as compared with the design criteria of MOC = 100 μB. The 32-μB discrepancy is attributed primarily to quality control problems in the mockup lattice.

TABLE XX

Rod Loadings in PDP Margin of Control Experiments

Experiment No. 1

Septifoils	Loading (rods in)
Central septifoil	E, B at 33.7 cm[a]
Gangs I and II	B, C, E, F[a]
Gang III	0.86" dia. Cd in A and B 3.5% Li in D and E[b]

Three targets in core (adjacent to Gang II septifoils)

Experiment No. 2

Septifoils	Loading (rods in)
Central septifoil	C, F, E at 85 cm[a]
Gang I and II	A, B, C, E, F[a]
Gang III	0.86" Cd in A and B, 3.5% Li in D and E[b]

One target in core (central hex)

(a) Rods in positions A, D, and G are 0.45-inch-diameter Cd, in positions B and F 0.35-inch Cd rods, and in positions C and E 0.27-inch Cd rods. C and F are partial length rods and are centered vertically in the core.

(b) The MOC is very insensitive to changes in the loading of Gang III septifoils. Changing from a two-rod loading to a seven-rod loading in Gang III results in a change in pile buckling of only 16 μB.

Δk Rod Measurements

A set of three special nickel Δk rods and a set of three conventional cadmium Δk rods were tested in the production high-flux charge in the PDP. The lattice locations in which the rods were tested, which in turn correspond to the proposed plant reactor locations, are shown in Figure 23.

The initial tests with the nickel Δk rods showed that they gave a prompt power increase of only about 1%, much too small an effect to be useful in the plant reactors. The nickel rods were therefore eliminated from further tests.

With the cadmium Δk rods a series of kinetics tests were made to (1) obtain by stable period measurements an accurate estimate

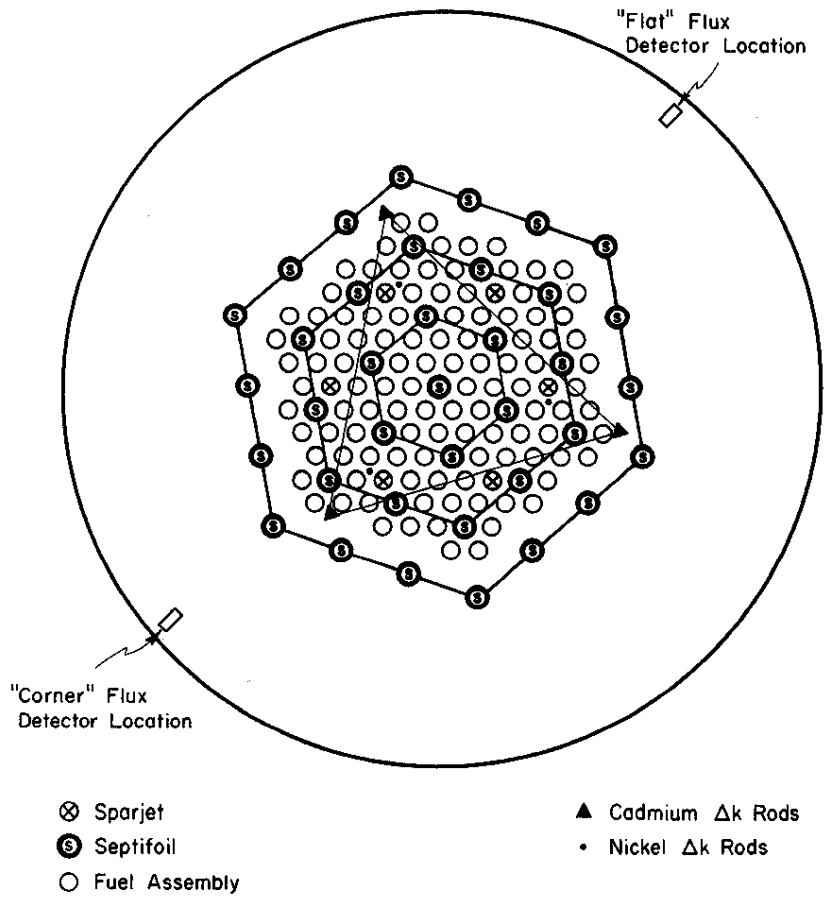

FIG. 23 Δk ROD LOCATIONS IN PDP PRODUCTION LATTICE TEST

of the reactivity worth of the Δk action, (2) obtain directly the prompt power increase obtained on rod action, and (3) determine the differences in response of flux detecting instruments at different locations around the pile.

Period measurements with the cadmium Δk rods were made in two pile loadings; one in which Gang III septifoils each contained 4 control rods, and another in which these septifoils were empty. In both cases the Δk rods were in the locations shown in Figure 23 and the rest of the control septifoils were uniformly loaded with four control rods. All Δk rod measurements were made at full moderator height, criticality being maintained as necessary by moving a rod in the central septifoil. In the period measurements, the pile power was leveled with the three cadmium Δk rods in the unshadowed (most poisonous) position. The rods were then actuated to the shadowed position (giving an increase in reactivity) and the pile power was allowed to increase on a stable period.

This period was obtained by monitoring the flux rise with several compensated ion chambers. Values of Δk_{eff} corresponding to the measured periods were obtained from a calculated period-reactivity relationship. The reactivity worth of the three rods was 0.04% $\Delta k/k$ in the case with four rods in each of the Gang III septifoils and 0.11% in the loading with no control rods in the Gang III septifoils. These values correspond to prompt power changes of 5.5% and 17.7%, respectively. The total reactivity worth of the three rods (i.e., the effect of completely removing the unshadowed rods from the pile) was 0.18% $\Delta k/k$ in the case with four control rods in Gang III.

Since the local change in reactivity introduced by the Δk rod action causes a flux shape change as well as an overall power change, flux detecting instruments in different locations may be expected to "see" different flux changes, particularly in the present case where the Δk rods are located so near the edge of the lattice. To determine the importance of this effect as well as to obtain a direct measure of the prompt power change, Δk rod kinetics tests were made with the flux detecting instruments in different locations around the pile. Two Westinghouse compensated ion chambers were used in each test. In some runs one chamber was located at the vertical midplane of the core facing a corner of the triangle formed by the three cadmium Δk rods and the other chamber was located facing a side of the triangle. In other tests one instrument faced the corner of the triangle and the second was on top of the pile at the center. Data from both instruments were obtained with a high speed strip chart recorder and from one of the instruments with the digitizing tape printout equipment normally used in plant Δk rod measurements. The data were recorded both during the power-increasing rod action (i.e., in moving from an unshadowed to shadowed position) and the power-decreasing action, and in each test the rods were recycled 3 to 5 times. Finally, the tests were made both with the Gang III septifoils loaded with 4 control rods and with them empty. The results for the cases in which Gang III septifoils contained 4 control rods are presented graphically in Figure 24, where the flux signals obtained from the different instruments are plotted as a function of time after rod activation. The flags on the experimental points represent the standard deviation of the mean of the 3 to 5 rod recycle runs in each test. It is obvious from these plots that the results of Δk rod measurements are strongly dependent upon the location of the flux detecting instruments.

In analyzing the results from the high speed recorders it was observed that the three Δk rods did not all actuate at the same time. For example in the cases where the rods were actuated to produce a flux increase, i.e., from unshadowed to shadowed position,

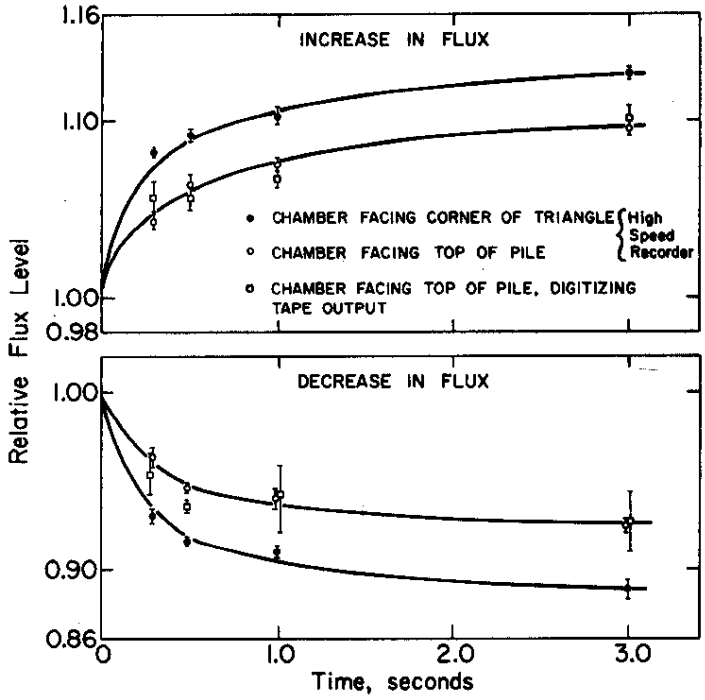

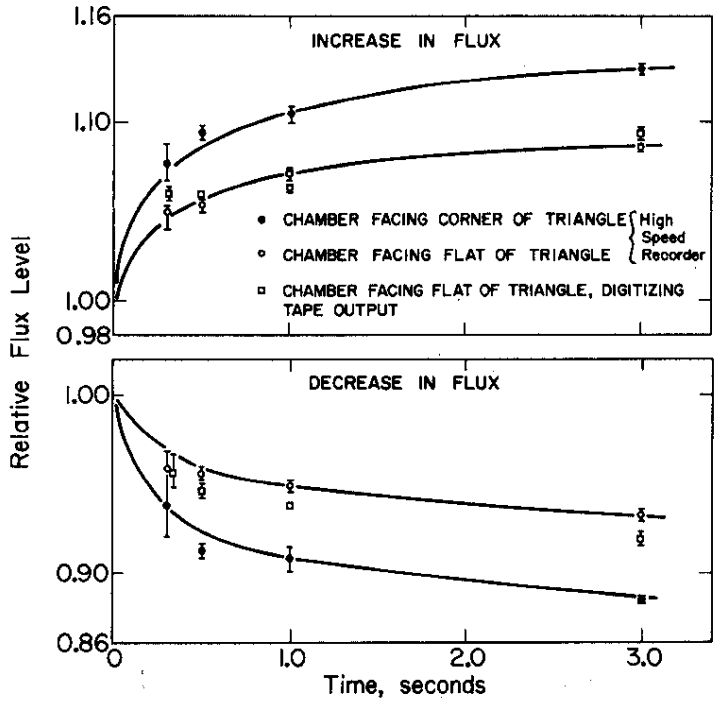

FIG. 24 FLUX PLOTS FROM PDP Δk ROD TESTS

the total elapsed time between the start of motion for the first rod and the start of motion for the last rod was 0.02 to 0.03 second. In these cases, the mechanical motion was in the downward direction. In the cases where the mechanical rod motion was in an upward direction, i.e., moving from shadowed to unshadowed position, the time span between start of motion of the first and last rods ranged from 0.12 to 0.19 second. Since the time of rod motion (in the up direction) is 0.23 to 0.27 second, the total elapsed time between initiation of rod motion and completion of all rod motion (total rod motion time) in some cases was as long as 0.47 second.

Under the assumption that the prompt power change is essentially complete at 0.5 second, the results in Figure 24 show that the flux detecting instrument facing the flat of the triangle formed by the three Δk rods gives the most nearly correct overall power response, i.e., about 5.5%, as was determined by the period measurements.

Table XXI summarizes all of the results of the experiment. The prompt power change given in each case was taken at 0.5 second, and in cases where both high speed recorder data and digitizing tape data were available the given result is an average of the two. It can be seen that in each test, the instrument facing the flat of the triangle or the instrument on top of the pile gives the better result. Table XXI also shows that the power change that has occurred 0.5 second after rod activation in moving from the

TABLE XXI

Results of Cadmium Δk Rod Kinetic Tests

Test	Rods in Gang III	Relation of Chamber to Δk Rod Triangle(a)	Direction of Power Change	Indicated Prompt Power Change, %(b)
1	4	Facing flat	Increase	5.5
			Decrease	5.0
		Facing corner	Increase	9.5
			Decrease	8.0
2	4	On top of pile	Increase	6.0
			Decrease	6.0
		Facing corner	Increase	9.0
			Decrease	8.0
3	None	Facing flat	Increase	18
			Decrease	14
		Facing corner	Increase	22
			Decrease	17

(a) See Figure 23.
(b) 0.5 sec after initiation of rod motion.

shadowed to the unshadowed position is in almost every case less than the corresponding change obtained in moving the rods in the opposite direction. The reason for this apparent difference is not known, since in no cases did the total rod motion time exceed about 0.5 second.

Production Control Rod Worths

The measurements of control rod worths that were discussed earlier were obtained with mockup cadmium rods with diameters approximating, but not identical to, the proposed high-flux charge control rods. Measurements using the actual production control rods were completed in the full production charge loading. The rod worths as they would occur in a flat flux together with the rod worths expected in the production high-flux charge are given in Table XXII. The particular rod combinations that were measured reflect various conditions that may occur during normal operation, or that are needed for control calculations.

TABLE XXII

Worths of Control Rods
Fabricated for High-Flux Charge

X denotes occupied position.

Rod Location[a]	A	B	C	D	E	F	G	Worth, μB	
Rod Size[b]	0.45	0.35	0.27[c]	0.45	0.27	0.35[c]	0.45	Flat Flux	High-Flux Charge
	X	X	X	X	X	X	X	896	925
	X	X	X	X	X	X	-	856	884
	X	X	X	-	X	X	X	825	852
	X	X	-	X	X	-	X	799	825
	X	X	X	-	X	X	-	763	788
	X	X	-	X	X	-	-	725	749
	X	X	-	-	X	X	-	680	702
	-	X	X	-	X	X	-	661	683
	X	X	-	X	-	-	-	648	669
	X	X	X	-	-	-	-	574	593
	-	X	X	-	X	-	-	536	554
	X	-	-	-	-	X	-	460	475
	X	-	-	-	X	-	-	452	467
	-	X	-	-	X	-	-	417	431
	-	-	X	-	X	-	-	379	392
	X	-	-	-	-	-	-	296	306
	-	X	-	-	-	-	-	248	256
	-	-	X	-	-	-	-	204	211
	-	-	-	-	-	-	-	0	0

(a) Conventional designation - Positions A through F clockwise around septifoil with G in center.
(b) Cadmium diameter, inches
(c) These were full length rods instead of partials that would normally occupy these positions.

Safety Rod Worth

The worth of the high-flux safety rod system was measured in the production charge in the PDP. The change in buckling resulting from the addition of 27 cadmium rods to the lattice (in the proposed safety rod positions) was determined by changing septifoil loadings as well as critical moderator height. The rods used were the standard high-flux 0.27-inch-diameter rods. Initial plans called for the use of 0.21-inch-diameter rods; their worth was so small, however, (particularly since three of them will be replaced with cadmium Δk rods) that they were changed to 0.35-inch-diameter rods. Table XXIII gives the total worth in $\Delta k_{eff}/k_{eff}$ of the safety system for all three rod diameters. The worths for the 0.21- and 0.35-inch-diameter rods were obtained from the worth of the 0.27-inch rod system by ratioing earlier rod worth data.

TABLE XXIII

Safety Rod System Worth - 27 Rods

Cadmium Rod Diameter, inch	ΔB_z^2, μB	$\Delta k_{eff}/k_{eff}$, %
0.21	175	5.3
0.27	214	6.6
0.35	259	7.9

The sparjets were measured with no rods in them and then loaded with 1% and 3.5% Li-Al rods. When six of these rods were inserted, one in each sparjet was found to lower the pile buckling 35 and 65 μB, respectively.

APPENDIX

CONTROL SYSTEM MANAGEMENT: by S. V. Topp

The Savannah River Plant control rod system, as used in the high-flux charge, is extremely flexible and powerful. One, therefore, has a number of choices of the mode of control rod operation. Detailed calculations of the effect of control system management on the charge, as a function of burnup, were necessary in order to make an intelligent decision on the operation of the charge. Two schemes of control rod withdrawal were investigated theoretically: uniform withdrawal of all rods and withdrawal preferentially from the center.

The lattice assumed in the calculations consisted of 19 hexes of fuel and control positions surrounded by a reflector, as shown in Figure 2. The fuel assemblies were assumed to be 6 ft long and to have the cross-sectional dimensions given in Figure 3; each fuel assembly was assumed to contain 25 g/ft of ^{235}U. The lattice contained six sparjets in the positions shown in Figure 2.

Two-dimensional heterogeneous theory was used to calculate for two schemes of operating the control system: (1) pile flux shapes at various times during a cycle, (2) pile power profiles at various times during a cycle, (3) fluxes in individual fuel assemblies as a function of time during a cycle, (4) integrated fluxes, average pile burnup, and other macroscopic parameters, and (5) cycle lengths.

The heterogeneous theory developed by Feinberg and Galanin[7] treats each assembly discretely as a line source and line sink of neutrons; the flux at a given assembly is obtained by summing the flux contributions at that assembly due to every assembly in the lattice using kernels derived from age-diffusion theory. Thus:

$$\gamma_n i_n = \sum_{m=1}^{N} \left(\frac{\eta_m}{k} F^*_{mn} - f_{mn} \right)_{i_m} \qquad n = 1,2 \ldots N \qquad (1)$$

where

γ_n = ratio of "asymptotic" thermal flux at the assembly surface to thermal neutron absorptions per unit length and time in the assembly. The "asymptotic" thermal flux is the flux calculated from Equation (1) and is determined by the moderator properties and the center-to-center distances between assemblies, but is independent of the detailed geometry and materials of the assembly

i_n = thermal neutron absorptions per unit length and time in the n^{th} assembly

N = total number of assemblies

η_m = fission neutrons produced per absorption in the m^{th} assembly

k = the effective multiplication constant of the pile

F^*_{mn} = fission-to-thermal source kernel giving the thermal flux due to an infinite line source at a distance from the source corresponding to the center-to-center separation distance of the m^{th} and n^{th} assemblies. F^*_{mn} includes a single resonance approximation to take into account fast absorptions by any assembly type.

f_{mn} = thermal sink kernel giving the thermal flux depression due to an infinite line sink at a distance from the sink corresponding to the center-to-center separation distance of the m^{th} and n^{th} assemblies

and where axial leakage is taken into account by inclusion in the moderator absorptions as described below. Table XXIV gives the form of the kernels used.

An IBM 704 computer code, HERESY I, was written by C. N. Klahr[6,8] et al. embodying the two-dimensional heterogeneous theory of Feinberg and Galanin[7]. HERESY, with some SRL modifications for ease of use, was used for the reactor calculations described herein. The following is a description of the physics input required for HERESY:

Moderator Properties

- L^2, the square of the thermal diffusion length - Axial leakage from the pile is accounted for by adjustment of L^2 so that

$$\frac{1}{L^2} = \frac{1}{L^2_{mod}} + B_V^2$$

where B_V^2 is the axial buckling of the pile and L^2_{mod} is calculated for the moderator only.

- Σ_a, the modified thermal absorption cross section -

$$\Sigma_a = \frac{D_{mod}}{L^2}$$

where D_{mod} is the thermal diffusion coefficient of the moderator.

TABLE XXIV

Single Resonance HERESY Kernel Functions

$$f_{mn} = \frac{1}{2\pi D} K_o\left(\frac{r_{mn}}{L}\right)$$

$$F^*_{mn} = F_{mn} - \sum_{t=1}^{N} A_t g_{mt}^{(E)} F_{tn}^{(E)}$$

where

$$F_{mn} = \sum_{i=1}^{3} \alpha_i \frac{e^{\frac{\tau_i}{L^2}}}{2\pi D} \left[K_o\left(\frac{r_{mn}}{L}\right) + \frac{\tau_i}{2L^2} e^{-\frac{r_{mn}^2}{4\tau_i}} - \frac{1}{2}\left(1 + \frac{r_{mn}^2}{4L^2}\right) E_1\left(\frac{r_{mn}^2}{4\tau_i}\right)\right]$$

($F_{tn}^{(E)}$ is obtained from the equation for F_{mn} by replacing τ_i by $\tau_i^{(E)}$ and by replacing r_{mn} by r_{tn}).

$$g_{mt}^{(E)} = \sum_{i=1}^{3} \frac{\alpha_i}{4\pi\tau_i(E)} e^{-\frac{r_{mt}^2}{4\tau_i(E)}}$$

and where r_{mn} is the perpendicular distance from rod m to rod n. D, L, A, α, τ, and $\tau^{(E)}$ are described in the text as giving Moderator Properties or Lattice Assembly Properties. E_1 is the exponential integral[8]. Superscript "E" denotes the energy dependence of the quantity involved. The energy of the single effective resonance can be changed by changing the corresponding τ values and kernels.

- α_1, α_2, α_3; τ_1, τ_2, τ_3; $\tau_1(E)$, $\tau_2(E)$, $\tau_3(E)$ - These quantities are parameters in a triple-Gaussian expression for the slowing-down density q from a line source to thermal or to the energy of some resonance:

$$q_{th} = \sum_{i=1}^{3} \frac{\alpha_i}{4\pi\tau_i} e^{-\frac{r^2}{4\tau_i}}$$

$$q_{res} = \sum_{i=1}^{3} \frac{\alpha_i}{4\pi\tau_i(E)} e^{-\frac{r^2}{4\tau_i(E)}}$$

It has been found experimentally at SRL that the slowing-down density to the indium resonance from an infinite line source in heavy water can be well-fitted with a double Gaussian formalism where $\alpha_1 = 0.560$, $\alpha_2 = 0.440$, $\alpha_3 = 0$, $\tau_1(E) = 147.9$ cm^2, $\tau_2(E) = 61.9$ cm^2, $\tau_3(E) = 0$ for 99.70 mol % D_2O at 22°C.[8] Corrections to these numbers are then made to obtain τ values to the resonance energy of interest, to the slow energy which is consistent with the energy range used to calculate L^2_{mod}, and for the desired moderator temperature.

The following parameters are needed for each assembly type, where assembly type is determined by physical composition and by location with respect to other assemblies. A maximum of 50 such types may be used with HERESY, and a lattice may be made up of many assemblies of each type.

- γ - Equation (1) has been solved for an infinite hexagonal lattice of one assembly type to obtain an expression for the calculation of γ, similar to the manner described by Klahr[8] for square lattices. Thus γ is given by:

$$\gamma = \frac{L^2_{mod}}{VD_{mod}} \left\{ \frac{1 - f}{f} - \frac{V}{4\pi L^2_{mod}} \left[2K_o\left(\frac{R}{L}\right) - \ln\left(\frac{L^2}{V}\right) - 2.8741 \right] \right\}$$

where f is the modified thermal utilization; i.e., the fraction of cell absorptions occurring in entire assembly.

- η -

$\eta = \epsilon$ [neutrons produced per assembly thermal absorption]

where ϵ is the fast fission factor.

- A - the resonance parameter for an equivalent lumped resonance,

$$A = \frac{1-p}{V}$$

where p is the resonance escape probability to thermal energies and V is the cell volume per unit length.

- R - the assembly radius.

- The Cartesian coordinates measured from the reactor center must be specified for each assembly.

The reactor characteristics given as output by HERESY are the normalized thermal and resonance absorptions for each assembly type, and pile averaged eta, resonance escape probability, thermal utilization, and reactivity.

Calculation of the Operating Characteristics

The operating characteristics of the high-flux reactor were calculated using the following method: Initially the nuclear properties of all fuel assemblies in the lattice were identical, and the control position absorptions were adjusted so that the reactor was approximately 50 μB subcritical, cold clean. The manner in which the control absorptions varied depended upon which of the two control schemes was used. For either case, new HERESY parameters for the assemblies and moderator were used corresponding to the hot-clean reactor with equilibrium Xe-Sm poisoning; the control absorptions were changed to give criticality in this state. From the HERESY results, the relative neutron flux in each fuel assembly was calculated from:

$$\phi_i = \frac{(ABS)_i}{\Sigma_{ai}}$$

where

ϕ_i = average relative neutron flux in assembly type i

$(ABS)_i$ = thermal absorptions in assembly type i as given by HERESY output

Σ_{ai} = macroscopic absorption cross section of assembly type i

The relative power in each fuel assembly was calculated from

$$P_i = \phi_i \Sigma_{fi}$$

where Σ_{fi} = macroscopic fission cross section of assembly type i. Σ_a and Σ_f were calculated with THERMOS as a function of ^{235}U concentration, with appropriate fission products and Xe-Sm.

The absolute assembly fluxes were obtained from the relative fluxes by choosing the flux in the assembly with the highest power to give that assembly a power of 8 MW. The flux in each assembly was assumed to be constant over some time interval (usually 1.5 days) which was small compared to the cycle length; the ^{235}U concentration at the end of such a time interval is given by

$$N_i(t + \Delta t) = N_i(t) e^{-\sigma_a \phi_i \Delta t}$$

where σ_a is the microscopic absorption cross section of ^{235}U, and $N_i(t)$ and $N_i(t + \Delta t)$ are the ^{235}U concentrations at the beginning and end, respectively, of the time interval Δt. σ_a was determined from THERMOS cell calculations for the fuel assembly and was found to be effectively constant over the range of ^{235}U concentrations of interest.

Given the new ^{235}U concentrations for each assembly type at the end of the first time interval, plots of the HERESY η and f as a function of ^{235}U concentration were used to obtain new HERESY parameters for each fuel assembly type. HERESY calculations were run with the new parameters, changing the septifoil absorptions to maintain criticality. Thus another series of assembly absorptions, relative fluxes, relative powers, absolute fluxes, etc. were obtained as described above for use in calculating the ^{235}U concentration of each fuel assembly, after another burnup time interval. This procedure was repeated until all the septifoils were empty and the cycle ended.

In this manner, the characteristics listed above were obtained for each of two schemes of withdrawing the control rods. The first of these consisted of withdrawing the rods uniformly from all the control positions shown in Figure 2 until all the rods were out and the cycle ended; the second scheme consisted of maintaining criticality throughout the cycle by first withdrawing all rods from the central septifoil, then withdrawing all rods from the ring of six septifoils, then from the next

ring of twelve septifoils, and finally from the septifoils in the reflector, at which point all the rods were out and the cycle ended. The results of using each of these schemes are given in the last section.

Figure 3 gives a cross section of the fuel assembly used. Each fuel assembly was assumed to initially contain 25 g/ft of ^{235}U. THERMOS calculations were made for this fuel over a range of ^{235}U concentrations corresponding to various burnup conditions. Fission products were assumed to have no burnup and were considered in the calculations to have 1/v absorption with a 0.025-ev absorption cross section of 50 barns per fission. At each ^{235}U concentration, the fuel was assumed to contain equilibrium Xe-Sm concentrations such that

$$(\Sigma_a \phi)_{Xe} = Y_{Xe+I}(\Sigma_f \phi)_{235}$$

and

$$(\Sigma_a \phi)_{Sm} = Y_{Sm}(\Sigma_f \phi)_{235}$$

where Σ_a and Σ_f are macroscopic absorption and fission cross sections, respectively; and Y is the total fission yield of the isotopes indicated. This approximate method of treating the Xe-Sm poisoning was used to help simplify the calculations to give plots of the HERESY parameters as a function of ^{235}U concentration only. Exact treatment is complicated by the fact that a given ^{235}U concentration is reached by different assemblies at different times, so that for a given ^{235}U concentration there is actually no fixed Xe-Sm concentration. Also resonance capture and fission were neglected for all fuel concentrations.

Septifoil

The HERESY input parameter γ cannot be calculated for the complicated configuration of rods in a septifoil because of difficulty in obtaining a value of f for such a configuration. Also the effective radius of a septifoil containing rods is not well defined. Therefore the septifoil absorptions were treated by assigning to the septifoil an arbitrary radius and by then varying γ_{sept} to maintain criticality as the fuel burned up. The septifoil γ's thus do not describe specific rod complements (except that γ for an empty septifoil is known from previous normalization to experiment); rather the calculations specify that if the control rods are pulled in the positions indicated enough to maintain criticality throughout the cycle, then the calculated cycle lengths, flux profiles, etc. follow.

Normalization was made to SE-PDP rod worth measurements in order to fix more closely the septifoil rod complement in terms of the septifoil thermal utilization, f_{sept}. These calculations were done with a FZ configuration of the fuel shown in Figure 3 for a moderator purity of 99.58 mol % D_2O and ^{235}U concentration of 20 g/ft. Infinite lattice HERESY with zero vertical buckling was used to calculate k for various values of f_{sept}; values of B_m^2 vs. f_{sept} were then obtained using age-diffusion theory. The previously normalized value of f_{sept} for an empty septifoil was used with the above results to obtain a plot of rod worth vs. f_{sept} and the SE-PDP measurements of rod worth for a wide range of septifoil loadings in a similar lattice were used to obtain the values of f_{sept} vs. rod loading shown in Table XXV. It

TABLE XXV

Septifoil Thermal Utilization from SE-PDP Normalization

Moderator purity = 99.58 mol % D_2O Moderator temperature = 20°C

$L^2_{mod} = 7.9197 \times 10^{a}$ $D_{mod} = 0.8096$

Control Rod Complement in Septifoil(a,b)							Thermal Utilization
A	B	C	D	E	F	G	
0.86	0.86	3.5% Li	0.86	3.5% Li	3.5% Li	0.86	0.99570
.86	.86	3.5% Li		3.5% Li	3.5% Li		.99455
.86	.86	3.5% Li					.99197
		3.5% Li					.9702
.625	.45	.25	.625	.45	.25	.86	.99528
.625	.45	.25		.45	.25	.86	.99439
	.45	.25		.45	.25	.86	.99322
	.45	.25		.45	.25		.99105
	.45	.25			.25		.98690
		.25			.25		.9774
					.25		.9550
.86	.45	.25	.86	.45	.25	.86	.99546
.86	.45	.25		.45	.25	.86	.99448
	.45	.25		.45	.25	.86	.99320
	.45	.25		.45	.25		.99103
.45	.25	.25	.435	.45	.25	.435	.99488
.45	.25		.435	.45		.435	.99368
.45	.25	.25		.45	.25		.99290
.45	.25			.45			.98984
	.25			.45			.98417
.45	.25						.98273
	.25						.9578
	Empty Septifoil						.70000

(a) See Figure 4.

(b) Except where noted all rods are cadmium with diameter given in inches.

should be emphasized that f_{sept} for a given rod loading is applicable only with the moderator properties shown in Table XXV; if other moderator properties are used, f'_{sept} should be used with a given rod loading such that

$$(1 - f'_{sept}) = (1 - f_{sept}) \frac{\Sigma_a}{1.0223 \times 10^{-4}}$$

where Σ_a is the macroscopic absorption cross section of the moderator.

As described in a previous section, the moderator properties required for input to HERESY are L^2_{mod}, D_{mod}, Σ_a, and the triple Gaussian parameters for the slowing-down density. L^2_{mod} and D_{mod} were calculated from the same 30-group THERMOS calculation made for the fuel, with averaged cross sections for the moderator region external to the fuel assembly. Although these moderator properties changed somewhat with ^{235}U concentration in the fuel, the moderator properties calculated with the fuel having initial ^{235}U concentration were used throughout a cycle. The triple Gaussian parameters were modified from those discussed in a previous section to give a value of $\tau_{thermal} = 117$ at 20°, which is reasonably consistent with the 30-group THERMOS calculations of L^2. Table XXVI lists the moderator input parameters.

TABLE XXVI

Moderator Input Parameters for HERESY

Moderator purity	99.70 mol % D_2O
Moderator temperature	90°C
L^2_{mod}	1.210×10^4 cm^2
D_{mod}	0.86058 cm
α_1	0.560 cm^2
α_2	0.440 cm^2
α_3	0
τ_1(th)	155.9 cm^2
τ_2(th)	68.3 cm^2
τ_3(th)	-
τ_1(30 ev)	126.5 cm^2
τ_2(30 ev)	40.5 cm^2
τ_3(30 ev)	-

Detailed pile flux calculations were made for two schemes of control system operation. Table XXVII gives the calculated cycle lengths and other characteristics for each scheme. PDP measurements of rod worth and buckling have indicated that the fuel concentration should be 22 g/ft ^{235}U in order to give the margin of control desired for the production reactors. It is estimated that such a fuel concentration would shorten the cycle lengths given in these calculations by approximately 2.5 days, since the calculations were done at 25 g/ft ^{235}U.

TABLE XXVII

High-Flux Cycles for Two Methods of Control Rod Withdrawal

Parameter	Control Rod Withdrawal Scheme: Uniform Withdrawal	Control Rod Withdrawal Scheme: Withdrawal from Center
Pile burnup, MWD	6140	5910
Average pile power, MW	680	510
$\int \phi dt$, Position 2,[(a)] n/cm^2	2.22×10^{21}	2.88×10^{21}
$\int \phi dt$, avg over pile, n/cm^2	1.32×10^{21}	1.26×10^{21}
Max ϕ, Position 2, n/(cm^2)(sec)	4.23×10^{15}	4.05×10^{15}
Avg ϕ, n/(cm^2)(sec)	1.70×10^{15}	1.20×10^{15}
Cycle length, days	9.0	11.5

(a) See Figure 19 for Position 2.

The results show that the highest point flux occurs toward the end of the cycle in the uniform-withdrawal case; the highest time integrated point flux occurs in the center-out withdrawal scheme; and the highest pile and cycle averaged flux occurs in the uniform-withdrawal case. Thus the uniform-withdrawal scheme is probably the better choice for a demonstration of overall high-flux operating ability, but withdrawal from center out would be better for sample irradiation in one or a few positions with a limited number of cycles.

REFERENCES

1. R. C. Axtmann and O. A. Towler, Jr. The Savannah River Exponential Facility. USAEC Report DP-49, E. I. du Pont de Nemours & Co., Savannah River Laboratory, Aiken, S. C. (1954).

2. A. E. Dunklee. The Heavy Water System of the Process Development Pile. USAEC Report DP-567, E. I. du Pont de Nemours & Co., Savannah River Laboratory, Aiken, S. C. (1961); J. L. Crandall. Status of the United States Effort in D_2O Reactor Physics. USAEC Report DP-787, E. I. du Pont de Nemours & Co., Savannah River Laboratory, Aiken, S. C. (1962); J. L. Crandall. Efficacy of Experimental Physics Studies on Heavy Water Lattices. USAEC Report DP-833, E. I. du Pont de Nemours & Co., Savannah River Laboratory, Aiken, S. C. (1963).

3. R. C. Axtmann et al. Initial Operation of the Standard Pile. USAEC Report DP-32, E. I. du Pont de Nemours & Co., Savannah River Laboratory, Aiken, S. C. (1953)(Declassified 8/29/57).

4. T. F. Parkinson et al. The Nuclear Test Gauge. USAEC Report DP-147, E. I. du Pont de Nemours & Co., Savannah River Laboratory, Aiken, S. C. (1956)(Confidential).

5. H. C. Honeck. THERMOS. A Thermalization Transport Theory Code for Reactor Lattice Calculations. USAEC Report BNL-5826, Brookhaven National Laboratory, Upton, N. Y. (1961).

6. W. R. Cadwell. PDQ-3 — A Program for the Solution of the Neutron-Diffusion Equations in Two Dimensions on the IBM-704. USAEC Report WAPD-TM-179, Westinghouse Electric Corp., Bettis Atomic Power Lab., Pittsburgh, Pa. (1960).

7. S. M. Feinberg. "Heterogeneous Methods for Calculating Reactors," Proc. U.N. Intern. Conf. Peaceful Uses Atomic Energy, 1st, Geneva, 5, 484-500 (1955). P/669; and A. D. Galanin. "Critical Size of Heterogeneous Reactor with Small Number of Rods." Ibid., 462-465 (1955). P/663

8. C. N. Klahr, L. B. Mendelsohn, and J. Heitner. Heterogeneous Reactor Calculation Methods. USAEC Report NYO-2678, TRG, Inc., Syosset, N. Y. (1960). (TRG-129-QTR-6)

9. C. N. Klahr, J. Heitner, and N. Stein. Test and Verification of Heterogeneous Reactor Calculation Methods - Annual Report - April 1963 - January 1964. USAEC Report NYO-3194-1, Fundamental Methods Associates, Inc., New York.

10. C. N. Klahr and L. B. Mendelsohn. Heterogeneous Reactor Calculation Methods. USAEC Report NYO-2674, TRG, Inc., Syosset, N. Y. (1959). (TRG-129-QTR-2)